Evidence of Quaternary and recent activity along the Kyaukkyan Fault, Myanmar

Author names and affiliations

Silvia Crosetto[1], Ian M. Watkinson[1], Soe Min[2], Stefano Gori[3], Emanuela Falcucci[3], Nwai Le Ngal[4]

[1] Department of Earth Sciences, Royal Holloway University of London, Egham, Surrey TW20 0EX, United Kingdom

[2] Department of Geology, Taungoo University, Bago Division, Myanmar

[3] Istituto Nazionale di Geofisica e Vulcanologia, Italy

[4] Department of Geology, Yangon University, Yangon, Myanmar

Corresponding author

Silvia Crosetto (silvia.crosetto.2013@live.rhul.ac.uk)

Abstract

Cenozoic right-lateral shear between the eastern Indian margin and Eurasia is expressed by numerous N-S trending fault systems inboard of the Sunda trench, including the Sagaing Fault. The most easterly of these fault systems is the prominent ~500 km long Kyaukkyan Fault, on the Shan Plateau. Myanmar's largest recorded earthquake, M_w7.7 on 23rd May 1912, focused near Maymyo, has been attributed to the Kyaukkyan Fault, but the area has experienced little significant seismicity since then. Despite its demonstrated seismic potential and remarkable topographic expression, questions remain about the Kyaukkyan Fault's neotectonic history.

In this study we document robust geologic evidence of fault activity along the Kyaukkyan Fault. Field investigation and interpretation of satellite imagery reveal deformation features developed along a fault system mostly indicative of Quaternary dextral strike-slip faulting.

Clearly defined tectonic geomorphology, including fault scarps and linear valleys, are used to trace the northernmost and southernmost part of the fault. The fault's central section is characterised by a complex pull-apart system, whose normal border faults show signals of relatively slow recent activity.

Dextral transtensional activity along the Kyaukkyan Fault is recorded by geomorphic features such as sag ponds, shutter ridges, offset and beheaded streams, triangular facets and low-sinuosity mountain fronts. The Quaternary age of activity is demonstrated by short-lived geomorphic features such as wind-gaps, offset and deformed alluvial fans, and even offset of man-made structures. In Inle basin, alluvial fan successions along the easternmost mountain front reveal a vertical transition from faulted and folded alluvial fan sequences adjacent to pre-Cenozoic flanking ranges, to overlying gravels that appear less deformed. Conversely, a locally buried cross-basin fault system has fresh geomorphic expression even within the uppermost parts of the lacustrine/fluvial basin fill. This may indicate Quaternary migration of dominant fault deformation from sidewall faults to a cross-basin fault system, which is indicative of a mature, high strain strike-slip fault and has been observed in other active strike-slip faults around the world and in analogue models.

Keywords

Kyaukkyan Fault, strike-slip, stream offset, tectonic geomorphology, Quaternary, active tectonics

1. Introduction

Strike-slip faults play an important role accommodating the northward movement of India and internal deformation within the Eurasian margins (e.g. Molnar and Tapponnier, 1975; Tapponnier et al., 1982; Le Dain et al., 1984; Vigny et al., 2003; Morley, 2009, 2013; Mohadjer et al., 2010). During the Cenozoic, the NE-directed movement of the Indian plate has resulted in northward motion of coupled India-western Myanmar relative to SE Asia (e.g. Curray et al., 1979), horizontal shortening along the northern Indian margin (e.g. Corfield and Searle, 2000; Yin and Harrison, 2000), subduction below western Sundaland (e.g. Hall et al., 2008) and lateral extrusion of blocks around the eastern Himalayan syntaxis (e.g. Tapponnier et al., 1982). The Shan Plateau, an elevated region of almost 1 km average elevation in eastern Myanmar, western Laos and part of NW Thailand, lies about 1000 km south of the eastern Himalayan syntaxis. It records evidence of both N-S and ENE-WSW trending strike-slip fault systems (Lacassin et al., 1998; Morley, 2004; Wang et al., 2014).

The northern Shan Plateau was struck by a large earthquake on 23rd May 1912 (Coggin Brown, 1917). The Kyaukkyan Fault, a N-S-trending ~500 km long strike-slip fault traversing the western Shan Plateau (e.g. Soe Min, 2010) is generally considered the fault that ruptured to produce the earthquake because of the distribution of isoseismals mapped soon after the earthquake and the fault's prominent topographic expression (Coggin Brown, 1917; Chhibber and Ramamirtham, 1934). The Maymyo (a colonial name for the modern city of Pyin-Oo-Lwin) earthquake, as it has become known, was initially estimated at magnitude 8 (Gutenberg and Richter, 1996), and more recently revised to M_s 7.7 to 7.6 (e.g Abe and Noguchi, 1983; Pacheco and Sykes, 1992). Wang et al (2014) re-evaluated the distribution of highest intensities together with the size of the earthquake, concluding that the 1912 event likely ruptured about 160 km of the northern section of the Kyaukkyan Fault.

Although there is modern strike-slip activity across the Shan Plateau, recently including the M_w 6.8 Tarlay event in 2011 (Soe Thura Tun et al., 2014), the Kyaukkyan Fault has been largely devoid of significant seismicity since 1912. Against this background there is a lack of detailed study into evidence of palaeoseismic activity from tectonic landforms and related Quaternary deposits. This paper reports field observations and interpretations of satellite images along the Kyaukkyan Fault that reveal distinctive geomorphologic and structural features, indicative of strongly transtensional deformation that occurred during the Quaternary. In this paper, we describe evidence for transtensional deformation from north to south with particular reference to the 1912 Maymyo earthquake that affected the northern segment (Fig. 1).

2. Geological setting

2.1. Tectonic framework

The Cenozoic tectonic evolution of Myanmar involves a complex interplay between subduction, collision, extension and strike-slip faulting, and is subject to continued debate (e.g. Lee and Lawver, 1995; Bertrand and Rangin, 2003; Searle and Morley, 2011; Hall, 2012; Morley, 2013; Ridd and Watkinson, 2013). From the Mesozoic to the Early Cenozoic, NE movement of the Indian plate resulted in the subduction of Indian oceanic crust beneath western Sundaland; convergence became increasingly oblique as the Indian plate rotated clockwise during the Cenozoic (e.g. Lee and Lawver, 1995; Curray, 2005). Subduction beneath Sundaland largely terminated in the Miocene (Mitchell, 1993; Hall, 2002; Curray, 2005), when the Indian continental crust became attached to the western part of Myanmar (e.g. Curray, 2005), detaching it from stable Sibumasu (Morley, 2009). The composite India-western Myanmar then moved progressively north relative to Sundaland from the Oligocene, along the Sagaing Fault and other structures (e.g. Bertrand and Rangin, 2003; Soe Thura Tun and Watkinson, 2017).

Paleogene transpression resulted in the development of a broad strike-slip fault network in Thailand and Myanmar, exemplified by the Three Pagodas fault zone and the Mae Ping fault zone (Lacassin et al., 1993, 1997; Morley et al., 2007; Morley, 2009). A series of fault systems related to the Mae Ping Fault are developed near its western end as it passes into Myanmar (Morley, 2004; Ridd and Watkinson, 2013; Fig. 1).

During the latest Paleogene, northward motion of India-western Myanmar resulted in a reversal of motion along the NW-SE trending strike-slip faults (Lacassin et al., 1997) and potentially further west in Myanmar (Bertrand et al., 1999; Bertrand and Rangin, 2003; Morley et al., 2007; Soe Min, 2010; Wang et al., 2014). Subsequently this process resulted in the localisation of dextral strain along the Sagaing Fault (Bertrand and Rangin, 2003; Soe Thura Tun and Watkinson, 2017). On the Shan Plateau in eastern Myanmar, there is evidence that E-W trending strike-slip fault systems changed from right-lateral to left-lateral (e.g. Holt et al., 1991; Lacassin et al., 1998; Wang et al., 1998; Shen et al., 2005; Socquet and Pubellier, 2005).

The modern convergence rate between India and Eurasia is about 41 mm/yr (Vigny et al. 2003). The N-S trending, right-lateral Sagaing Fault accommodates about half (18-20 mm/yr) of this northward motion (e.g. Vigny et al., 2003; Socquet et al., 2006). The residual motion is considered to be accommodated in the Indo-Myanmar Ranges and the West Andaman fault system and potentially also within the Shan Plateau (Vigny et al., 2003; Sahu et al., 2006; Fig. 1).

2.2. Geology of the Shan Plateau

The Shan Plateau is underlain by Precambrian metasediments and a lower Paleozoic dominantly siliciclastic sequence overlain by Paleozoic carbonates (Chhibber and Ramamirtham, 1934); above this succession there are Permo - Triassic carbonates (Mitchell et al., 2012; Win Swe, 2012). Locally, marine clastics, carbonates and continental red beds

119 are found above the Permo - Triassic limestone. The western margin of the plateau is marked
120 by Upper Carboniferous to Lower Permian slates (Mitchell et al., 2002, 2007). The Shan
121 Plateau descends into the Myanmar Central Basin in the west, and this transition is marked
122 by outcrops of the Mogok Metamorphic Belt (e.g. Searle and Haq, 1964; Mitchell et al., 2007;
123 Searle et al., 2007). Many of these units were deformed during the Late Triassic Indosinian
124 Orogeny, during events related to the Late Cretaceous-Paleogene Andean-style margin of
125 Sundaland, and during Neogene indentation and gravitational collapse tectonics (e.g. Sone
126 and Metcalfe 2002; Bertrand & Rangin, 2003; Searle et al. 2007; Morley 2009), and thus
127 contain a plethora of pre-existing tectonic fabrics.

128 Cenozoic and Quaternary sedimentary rocks of the Shan Plateau have not been thoroughly
129 described in English-language literature. Quaternary sediments comprise lacustrine, fluvial
130 and alluvial fan deposits, and recent alluvial deposits (e.g. Win Swe, 2012).

131 **2.3. Previous studies of the Kyaukkyan Fault**

132 Although recognised early in the 20th Century (La Touche, 1913; Chhibber and Ramamirtham,
133 1934), the Kyaukkyan Fault remains poorly known. It was alluded to as part of a system of
134 'nested duplexes' by Morley (2004) and was more fully described by Soe Min (2010) and Soe
135 Min et al (2017). Recent studies (e.g. Wang et al., 2014) considered the seismic potential and
136 finite displacement along the fault. Two major rivers, the Myintnge and Thanlwin rivers (Fig.
137 1a), are offset as they cross the Kyaukkyan Fault. The hairpin loop geometry of the Myintnge
138 River south of the Nawnghkio Plateau is considered to record 5.3 ± 0.8 km right-lateral offset
139 (Soe Min et al., 2017). Restoration of this offset leaves about 10 km of left-lateral deflection,
140 interpreted by Wang Yu et al. (2014) as recording an earlier sinistral phase of the Kyaukkyan
141 Fault, though there are significant kinematic difficulties associated with this interpretation
142 (Soe Min et al., 2017). South of Inle lake at Hpansang, the Thanlwin River is reported to be
143 offset dextrally by 6.4 ± 1.0 km (Min et al., 2016), although in this section the river is not well

144 constrained by the topography, and the total dextral offset along the Kyaukkyan Fault
145 remains poorly constrained.

146 3. Data and methods

147 This study is based on field and remote sensing observations, combined to identify
148 geomorphic features that can record Quaternary and recent activity along the Kyaukkyan
149 Fault. These data are used to determine if the fault is active and capable of generating
150 ground-breaking ruptures (Machette, 2000; Galadini et al., 2012) associated with large
151 historical earthquakes like the 1912 Maymyo earthquake.
152 Shuttle Radar Topography Mission (SRTM) digital topographic data with 90 m and 30 m
153 spatial resolution and ASTER Global Digital Elevation Model (GDEM) with 30 m spatial
154 resolution were analysed using ArcGIS software. High-resolution visible spectrum satellite
155 imagery compilations freely available via Google Earth (including 2.5 m SPOT and 1 m
156 DigitalGlobe data) and the ESRI World Imagery compilation were used for detailed
157 geomorphic analysis (source: ESRI, DigitalGlobe, GeoEye, i-cubed, Earthstar Geographics,
158 CNES/Airbus DS, USDA, USGS, AEX, Getmapping, Aerogrid, IGN, IGP, swisstopo, and the GIS
159 User Community). The ESRI World Imagery highest resolution data has limited coverage in
160 some parts of the study area.
161 For this analysis we considered conventional geomorphic features which are discussed in the
162 text and summarised in Fig. 2a-e. These are:

163 - a) Inherited metre- to kilometre-scale offset and deflection of drainage along basin-
164 bounding faults (fault A in Fig. 2a), and minor offset of markers including man-made
165 structures along active intrabasinal faults (fault B in Fig. 2a) that are not crossed by
166 major river systems;
167 - b) Planar fault scarps with triangular facets, indicative of an active mountain front;

- c) Lineaments within unconsolidated sediments. Such features may result from ejection of fluids or fluidised sediments along a fault trace/surface rupture within basinal lacustrine sediments;
- d) Water and wind gaps, resulting from local uplift;
- e) Sharp fault contact between bedrock and alluvial fans, indicative of a syn-tectonic deposition of the alluvial fan succession.

4. Evidence of Recent and Quaternary activity along the Kyaukkyan Fault

Results from remote sensing and field observations are described below, arranged geographically from north to south along the Kyaukkyan Fault.

4.1. Kyaukkyan area

4.1.1. Kyaukkyan village railway bend

The northern 110 km-long, linear segment of the Kyaukkyan Fault, between Kyaukkyan village and 20 km north of Yawksak, is made of continuous fault segments each up to 30-35 km long, partly expressed as the steep west-facing topographic scarp of Nawnghkio Plateau.

At Kyaukkyan village a N-S trending limestone ridge marks the position of the long-lived geologic trace of the Kyaukkyan Fault. A small scarp marks the transition from the bedrock to the alluvial plain, occupied by cultivated fields. East of the limestone scarp, the Mandalay-Lashio railway runs along a man-made embankment standing ~2 m higher than the surrounding topography.

Coggin Brown (1917) reported damage caused by the May 1912 earthquake near Pyin-Oo-Lwin. He stated:

"*The line was only damaged to the east of Maymyo on the plateau itself, where it crosses the great Kyaukkyan Fault. [...] The railway lines were bent into a smooth curve close to the actual line of the fault, while cuttings and earth banks in the vicinity had slipped and blocked the line*".

At this site we observed that the railway smoothly bends to the right with a maximum deflection of 2.0 ± 0.2 m (Fig. 3). The bend starts at the bedrock scarp and deviation from the straight railway line continues eastward for ~100 m. The bedrock, characterised by Paleozoic grey limestone, shows intense fracturing and faulting in all outcrops observed along the ridge. Deflection of other man-made features such as the railway embankment and other earthworks in the proximity of the bend cannot be demonstrated. In a field north of the railway line there is a weak N-S trending topographic relief. One kilometre north of the bend, elongate subsiding areas of circa 100 m^2 are N-S aligned. Similar structures are observed along a subparallel N-S trend, 0.5 km further east.

Although the railway bend has commonly been attributed to the May 1912 earthquake and considered to support recent activity along the Kyaukkyan Fault (Coggin Brown, 1917; Wang et al., 2009, 2014; Soe Min, 2010), it is unclear whether the railway curvature is man-made (i.e. pre-dates the earthquake) or is tectonically-induced.

4.1.2. Gelaung valley

South of Kyaukkyan village, the west facing scarp of Nawnghkio Plateau is characterised by systematic river offsets along fault lineaments at the scarp's base in the Gelaung Valley (Fig. 4a). Most reliable offsets are associated with a shutter ridge between latitude N22°7' to N22°5' (Fig. 4b), where the cumulative offset is given by subsequent captures of upstream channels flowing from the plateau by a downstream channel moving to the north over successive stages.

Where there are no shutter ridges, it is more difficult to quantify the offsets with confidence: when the offset is smaller than the stream spacing, the deviation of the stream corresponds to the finite slip; however, if the offset is bigger than the spacing, the upstream section of a channel can be captured when the downstream section of another channel becomes aligned with it.

To quantify the strike-slip displacement along this section of the fault, stream offset restoration was applied along the Nawnghkio Plateau scarp, and is described in the following section.

Gelaung valley stream restoration

Stream offset restoration is a statistical technique used to determine strike-slip offset from tectonically deflected streams (e.g. Wallace, 1968; Replumaz et al., 2001; Fu et al., 2005).

The preservation of a stream offset depends on processes that are directly related to tectonic movements, but also subsequent processes like sedimentation and erosion. This technique is limited by the following conditions:

- the original streams might not have been straight;
- erosion can straighten deflected streams;
- offset can be obliterated if the slip is bigger than the streams spacing, as the truncated upstream will be captured by a beheaded downstream moving on the opposite side of the fault.

We assumed that the streams were straight before deflection, and left-lateral offsets were considered as apparent left-lateral offsets due to capture.

In order to perform the restoration, a map of all significant streams along the fault scarp was produced at 1:25,000 scale (Fig. 4b) using ESRI World Imagery.

A quantitative offset restoration was performed by shifting the block west of the Kyaukkyan Fault toward the south at scale increments of 25 m, and channels on either side of the fault were matched (Fig. 4c). The chart in Fig. 4d shows a random distribution of all matching streams for 0 to 1600 m restoration, and lacks a clear best match peak.

A qualitative restoration of 28 selected deflected streams to a simple straight watercourse shows a peak at 125 m restoration, followed by a wider best match distribution at 100 m and 175 m (Fig. 4e). These selected streams were manually chosen to avoid those that appear to record sequential capture events or have other anomalies that affect the apparent displacement recorded.

4.2. Indaw area

The Kyaukkyan Fault trace marks the topographic break between the western mountain front and Indaw basin west of the Zawgyi reservoir.

Parallel to the mountain front, Zawgyi River flows north approximately along the fault and then sharply bends westwards across the fault (Fig. 5a). The thalweg of the river is moderately sinuous with some meanders along much of this section, but flows straight and parallel to the fault for 800 m before crossing it with a turn to the west. A tilting of the basin, possibly caused by the active fault strand in the west, might have forced the river to shift toward the mountain front, where the thalweg assumed a straight course. Rather than a tectonic offset, the bend to the west appears as the preservation, west of the fault, of the original watercourse after southward migration of the upstream section lying east of the fault.

The northernmost river valley in Fig. 5b is deflected along a N-S trending ridge that might represent the master strike-slip partition in this section. The river-cut section through the

ridge exposes Permo-Triassic limestone cut by fault planes dipping 50° E, with a normal sense of motion given by calcite slickenfibre steps. In the riverbed, coarse, poorly sorted, apparently undeformed conglomerates unconformably onlap the bedrock.

Between Zawgyi River and the mountain front there is evidence of a deflected paleo-river (Fig. 5b). A linear feature is defined by a continuous, straight, sharp change in colour, parallel to the N150 trend of the fault. The light-coloured sediment is light-grey (fluvial?) sand filling an abandoned riverbed that runs southwards parallel to the mountain slope, and then sharply turns east to join the Zawgyi River. Darker *terra rossa* red sediment covers the surrounding higher topography. About 200 m of right-lateral offset separates the northern end of the feature from modern drainage, suggesting possible beheading of the downstream. Along the same mountain front there are abundant small modern streams that are beheaded (Fig. 5c) or deflected by amounts similar to those in the Gelaung valley, described above.

4.3. Inle Lake basin

4.3.1. Basin overview

Inle basin is part of a system of nested transtensional basins near the western margin of the Shan Scarp (Morley, 2004) that are associated with the Kyaukkyan Fault. Inle basin itself has the rhombic shape characteristic of a pull-apart basin (e.g. Dooley and McClay, 1997), defined by right-stepping strike-slip fault segments and associated normal faults.

The basin is about 130 km N-S and 40 km E-W in size. Along the Inle basin margins, there is considerable topographic relief focused along a series of apparently normal faults dipping in towards the basin. These generally have rounded, deeply incised morphologies inconsistent with recent rapid tectonic activity.

The main basin-bounding faults are the Pindaya normal fault on the west and the Taunggyi normal fault on the east (Soe Min et al., 2016; see Fig. 1 and Fig. 6a). Between the bounding

faults, a ridge parallel to the Pindaya Fault defines two sub-basins characterised by different drainage networks. The easternmost and bigger basin hosts Inle Lake.

The Inle Lake basin is about 100 km long in a N-S direction, and less than 30 km wide (Fig. 6a). Unlike other lakes developed within pull-apart settings/ basins of similar evolution and size (Lake Hazar, Timm et al., 2013; Mapam Yumco, Wang et al., 2013), Inle Lake, which occupies the deepest part of the basin, is surprisingly shallow: Sint and Catalan (2000) reported 4-6 m depth while, more recently, Sidle et al. (2007) measured the maximum depth as less than 4 m. The thickness of the sediments filling the basin is unknown, as well as the sedimentation rate; estimations are difficult due to the intense in-lake and near-lake agricultural practices.

The flat bottom of the Inle Lake basin shows some evidence of active or recent deformation, characterised by intra-basin uplift features. Pauktaw ridge emerges approximately 70 m above the basin floor (Fig. 6a) ~12 km west of Taunggyi. The calcareous sandstone exposed on the hill shows gently folded bedding, with N-S-trending fold-axes plunging to the south.

Similar uplifted structures are the Yebu and Sao-maw ridges, observed in the southern lake formed by the Mobye dam (Fig. 6b). These remarkably straight ridges are aligned and elongated along a N-S trend, giving a good constraint in the positioning of the fault in this otherwise low-lying area. Hot springs along the lineament might also suggest the presence of a steeply dipping conduit.

The position of the Kyaukkyan Fault is better constrained in the south, on the Myanmar-Thailand border, where a hairpin loop of the Thanlwin River records 2.3 ± 0.1 km of right-lateral offset along the fault (Fig. 7a, b). The river is confined to a narrow canyon and cannot avulse, making the estimate of river offset much more robust than previously reported at Hpansang (Soe Min et al., 2017).

4.3.2. Taunggyi area

The prominent Taunggyi scarp is located on the eastern side of the Inle Lake basin. The city of Taunggyi lies 400 m above the lake base level, on one of a series of structurally-controlled terraces delimited by two major and several smaller west-dipping scarps (Fig. 6a).

The prominent westernmost scarp cuts the Paleozoic limestone, which contains siltstone layers and shows wavy lamination. On fault planes at the top of the Taunggyi plateau, horizontal calcite slickenfibre steps in the Paleozoic limestone indicate pure strike-slip, and a right-lateral sense of motion. At the top of the scarp the limestone bedding dips variably east, increasing from 30° to 45° moving downslope, while toward the bottom of the scarp the limestones dip-angle is over 60° and normal, interbedding dip-slip is evidenced by slickensides. Generally, the bedrock is cut by open tension fractures dipping toward the west.

The westernmost Taunggyi scarp is characterised by poorly developed triangular facets, which are clearest along the southern part of mountain front (see Fig. 2b).

While dip-slip displacement along the margins of the Inle basin is clear from the topographic expression of the Taunggyi fault system, there is evidence for pure strike-slip with subtle topographic expression along a linear trend through the centre of the basin. Within the Inle basin north of Taunggyi, the Heke and Htedaung ridges delimit a drainage basin of about 50 km^2 bounded to the east by the mountain front (see Fig. 6a). Directly along strike to the north of the western Taunggyi fault scarp, a series of N-S trending lineaments occur within the basin fill.

Closest to the major basin-bounding scarp, a 1 m high gentle scarp delimits a flat area lying above the modern basin to the west. The scarp puts into contact the *terra rossa*, inferred to be an alteration product overlying shallow buried banded limestone, with the grey basin-filling silt. The scarp seems to be the expression of a fault synthetic to the basin-bounding fault in the shallow subsurface (see Fig. 2c).

Around 100 m west of and sub-parallel to the *terra rossa* margin, an anomalously sharp N-S trending contact 500 m long between lighter and darker basin filling silt can be observed in the field and in a 2012 Google Earth image (Fig. 8a, b). Linear vegetated patches lie along the trend for about 4 km.

Both light and dark silts are organic-rich and contain abundant gastropod shells. Silts with higher water content are darker than dryer silts. Water springs were found along the trend of the lineament at the margin of vegetated areas. The water pattern is not controlled by the topography and surface drainage, as the lineament has no topographic expression (see Fig. 2c).

4.3.3. Nampan area

South of Taunggyi, the Inle Lake basin has an average width of 6 to 10 km. In this narrow part, the western mountain front is deeply incised, has a gentle slope, and wide alluvial fans extend toward the lake over an area up to 50 km^2. The eastern basin-bounding fault scarp is steeper, has a sharp break of slope at its foot and alluvial fans extend over a smaller area of maximum 3km^2 (see Fig. 6a).

The geometry of alluvial fans is normally controlled by climate and tectonic activity, including changes in base-level and sediment supply, depending on both climate and the nature of the bedrock (Nichols, 2009). It is unlikely that climate varies significantly between the western and eastern ranges, and a change in the Inle Lake base-level would affect the hydrographic network to the same extent on both sides of the basin. The difference of shape and size of the alluvial fans observed around Inle Lake is most probably controlled by a combination of different sediment supply and different tectonic activity occurring at the front of each range. This conclusion is consistent with geomorphic evidence of greater tectonic activity along the eastern mountain front.

East of Nampan village, a 13 km^2 alluvial fan system is made of at least two recognisable alluvial fans, currently highly vegetated and cultivated, most likely formed by a single river as it exits the NE-SW trending valley east of Nampan (Fig. 9a, b). The apex of the southern fan is topographically higher than modern drainage exiting the valley, and it has no clear distributary channels. For these reasons it is considered to be older than the northern fan. The older alluvial fan has a SW long axis and paleo-flow direction.

The younger fan progrades significantly further into the basin than the older fan, and it is entrenched into the older deposit, suggesting a negative change in base-level (Bowman, 1978). This could be due to variation of base-level of the shallow Inle Lake, but is more likely a consequence of sustained uplift at the mountain front and/or uplift of the southern Inle Lake area (Fig. 9c; e.g. Pope and Wilkinson, 2005). The younger fan is cut by a 1 m high N-S striking scarp where it crosses the mountain front, suggesting tectonic activity during fan evolution.

In terms of recent fault activity, the two hills observed south of Nampan village, which pop-up in the southern part of the alluvial fan system (Fig. 9b), are significant. The hills are 10 m higher than the surrounding topography, and cover an area of approximately 1.3 km^2. They are divided by a water-gap extending in an E-W direction for 700 m. On the northern, smaller hill, a N-S-oriented road-cut exposes a succession of medium to fine sand with an intermediate layer of gravels composed of sub-rounded pebbles of sandstone and limestone, 2 cm to 15 cm in size; the biggest pebbles, 10-15 cm in diameter. Pebble imbrication indicates paleoflow towards the WSW. The gravel layer is 60 cm thick and 30 m wide. It has a lenticular shape, with a flat base and convex top, and is interpreted as a stream flow deposit. Stream flow deposits normally have a concave base and flat top (Reading, 2009), so the convex top of this deposit suggests that it has been domed upwards (see Fig. 2d).

381 The upstream (eastern) section of the water-gap is defined by a very gentle counter-slope
382 dipping toward the east. The lake-facing (western) side of the southern hill has an average
383 slope of 3.5%, except for a steeper section which forms a rounded scarp; this scarp lies along
384 the same trend as the 1 m scarp observed on the younger and northernmost alluvial fan
385 surface. The total length of the topographic scarp is over 4 km, bridging the entire valley
386 between the basement uplifts to the north and south.

387 The bisected ellipse shape of the two hills suggests that they might have been a single
388 landform gradually eroded by a stream flowing to the west. Then the stream changed its
389 course, leaving the modern water gap (Fig. 9c).

390 Stream deflection could be the direct consequence of uplift along a trend perpendicular to
391 the alluvial fan axis, which is supported by the stream flow deposits, currently on top of the
392 northern hill that have a domed geometry. When stream erosion does not keep pace with
393 uplift rate, a counter-slope forms and the stream is defeated, leaving a wind-gap in the
394 abandoned river course (e.g. Burbank et al., 1996; Delcaillau, 2001; Fig. 2e). The modern
395 creek flowing through the gap is too small to have eroded it, and its course is likely to have
396 been forced or modified by human activity.

397 The formation of the hills at Nampan is here explained using the lateral fold growth of folds
398 theory by Burbank and Anderson (2001). They consider folds connected to a subsurface blind
399 thrust. As the fault grows laterally, so does the fold that is its superficial expression: the fold
400 has, as a result, doubly plunging terminations with a structural saddle marking the zone of
401 linkage. This interpretation would explain the separation of the hills, and is supported by the
402 evidence of compression observed in Deposit F of Nampan quarry, described below.

403 ***4.3.3.1. Nampan quarry type locality***

404 Just north of Nampan, at the mountain front, Nampan quarry (visited during 2014-2016)
405 exposes narrow slices of intensely fractured micaceous and sub-vertically bedded quartzose

406 sandstone (see Fig. 11a), interpreted to be related to strike-slip fault activity at the mountain
407 front. The bedrock assemblage is overlain to the west by two sequences of alluvial fan
408 deposits separated by an unconformity. These deposits are sub-horizontal and tend to flatten
409 over the modern base level, suggesting a Quaternary age.

410 At the time of observation, Nampan quarry was a good site to observe tectonically
411 influenced, irregular alluvial fan sequences (e.g. Blair and McPherson, 1994; Harvey et al.,
412 2005; Fig. 2e) thanks to excellent fresh exposures. Schematic serial stratigraphic logs of the
413 alluvial fans are presented in Fig. 10; sedimentary environments are described in the
414 following section, based on generic sedimentary environments defined by Reading (1996)
415 and Nichols (2009).

416 *Alluvial fan depositional environments*

417 Deposit A

418 Within the Nampan alluvial fan exposures, the northernmost sequence, Deposit A (see Fig.
419 10) is a clastic body that extends from the mountain front almost to the lake shore. In the
420 apex, the clast-supported breccia corresponds to a talus facies deposited at the bottom of a
421 steep paleoslope interpreted as a newly-formed, fault-related scarp (see Fig. 2e), undergoing
422 erosion through weathering and gravity processes. Downslope, tabular breccia with metre-
423 scale blocks represents short transport of a catastrophic flow down a high angle slope (Fig.
424 11b): this is consistent with steep slope evolution in a humid, thinly vegetated environment.
425 The irregular contact between this deposit and the bedrock is an onlap unconformity above
426 which sediments are undeformed, suggesting that the alluvial fans were deposited on an
427 irregular paleotopography during a period of tectonic quiescence along the mountain front.

428 Within the distal part of Deposit A, poorly consolidated clastic sediments dipping 55°, much
429 steeper than the maximum 45° angle of repose considered for wet sand (Kleinhans et al.,

2011), may result from tectonic steepening, and are in contact with sub-horizontal sediments below, inferred to be older (Fig. 12a, b).

Deposit B

As for the previous deposit, the older part of Deposit B lies unconformably above an existing faulted basement paleotopography. Above the unconformity, the upper conglomerate shows cross-bedding lamination typical of stream flow deposits. In the distal part, horizontal stratification is due to flood deposition, where variable grain size reflects periodic flood cycles.

Deposit C

Deposit C has a different relationship with the faulted basement, being juxtaposed against it by a sub-vertical contact which could be related to Quaternary faulting (see Fig. 2e). The alluvial fan is characterised by prevalent stream flow facies: this type of flow erodes and reworks previous sediments and forms clast-supported conglomerates and pebbly sandstones as channel-fill deposits. Deposit C clearly exposes a prominent unconformity between the alluvial fan sequence directly in contact with the basement and poorly consolidated channelised breccias and sheet sands above. An apparent discontinuity, perhaps a fault, in the well bedded lower sequence is sealed by the unconformity and the overlying conglomerates filling an eroded channel (Fig. 12c, d).

Deposit D

The lower sequence of Deposit D characterised by a gravelly sand unit overlain by a channelised conglomerate (Fig. 10). One of the conglomerate channels is offset by a N-S trending fault and shows an apparent vertical offset of 50 cm (Fig. 12e, f) that is not clearly visible in the underlying gravelly sand. The absence of a consistent vertical offset in the two units precludes interpretation of dip-slip movement along the fault, suggesting instead strike-slip offset of the channel-fill deposits. The geometry of the offset involves right-lateral strike-slip for a north-plunging channel, and left-lateral strike-slip for a south-plunging channel; however, due to the position of the channel on the road cut, it was not possible to determine its dip direction. An E-dipping, possibly reverse fault appears to offset the gravelly sand by 20 cm.

The upper sequence is dominated by stream flow facies. Both upper and lower sequences of the fan are in sharp contact with the bedrock in the east. Gradual rotation of clasts from horizontal into parallelism with the sub-vertical contact of the upper conglomerate is interpreted as consequence of fault drag due to dip-slip movement along the surface that separates the two lithologies (Fig. 12g, h).

Based on the current topography, the stream responsible for the deposition of the sequences that comprise Deposit D seems to be beheaded: the current upstream drainage is almost non-existent, and the transport capacity is not proportional to the size of Deposit D. At the up-dip apex of the deposit, a N-S trending shutter ridge, which is slightly oblique to the Kyaukkyan Fault at this location, deflects the stream flowing along that valley by almost 500 m to the left. Strike-slip faulting might have caused the formation of the shutter ridge. The traces of dip-slip motion recorded as steeply-dipping clasts close to the Quaternary deposits-bedrock contact, and the elevation of Deposit D compared to Deposit E (described below), are evidence that uplift occurred, possibly related to the ridge formation.

476 Deposit E

477 This sequence shows features typical of sheet flood facies, with imbricated pebbles floating
478 in a fine-grained matrix (Fig. 11c), deposited during intense water flow following a rainy
479 period. It is topographically lower than the northern one by several tens of metres, and the
480 fluvial erosion forming the valley cannot explain this difference, which requires the
481 occurrence of one or more tectonic events. Although the relationship between this unit and
482 the prominent unconformity is not exposed, we interpret the unit to be part of the lower
483 sequence based on the lack of characteristic coarse conglomeratic material.

484

485 Deposit F

486 Deposit F clearly exposes a prominent unconformity between two sequences. The lower
487 sequence is composed of 3 units: at the base, F1, an ochre or reddish muddy siltstone; F2, a
488 channel fill conglomeratic body above a minor unconformity that locally completely removes
489 unit F1 and places F2 directly on the bedrock; F3, a white-pink to red gravelly siltstone with
490 layered concretions, conformably above F2. The layered concretions represent the
491 intermittent deposition typical of arid settings when some areas of the fan are starved of
492 sediment for long periods. In such conditions *in situ* alteration during pedogenesis or
493 weathering forms iron-oxide rich horizons. Unit F3 displays a stratigraphic pinch-out in the
494 distal part of the deposit.

495 Above the prominent unconformity the upper sequence is composed of poorly consolidated
496 channelised conglomerates.

497 This deposit shows characteristics of a gravity-flow fan: stream flows characterise unit F2
498 and, at a smaller scale, the sandy units; thick overbank deposits are represented by the fine-
499 grained units F1 and F3.

All three units of the lower sequence show evidence of syn- and post-sedimentary deformation in the middle part of the fan (Fig. 12i, j). A gentle fold has wavelength of 25 m assuming the hinge line is normal to the exposure, deforms parallel-bedded unit F2 and appears to have grown synchronously with unit F3, as demonstrated by the thinning of F3 layers over the fold apex. The unconformable contact between the lower sequence (units F1-F3) and the upper conglomeratic sequence is not visibly deformed. This provides a robust constraint on the timing of deformation: synchronous with deposition of unit F3 and prior to deposition of the upper unit.

Although a major fault that might explain the gentle folding of the lower sequence is not exposed, the succession is faulted in the mid part of the deposit. The intensely deformed micaceous bedrock is capped by a complete, intact weathering profile which, together with overlying units F1 and F2, shows ≈70 cm of apparent vertical offset. The fault plane is well defined but does not seem to continue into unit F3, where only lowermost concretion layers are gently folded, suggesting that the main movement causing offset took place during or after unit F3 deposition started.

A conspicuous feature of the lower succession in Deposit F is the presence of a chaotic conglomeratic body that interrupts the sedimentary layering of unit F2 (Fig. 12i, j; Fig. 11d). The conglomerate is composed of poorly sorted gravel to cobble sized clasts of quartzose sandstone and micaceous slate clasts in a coarse sand matrix. Against the irregular margin of this body lamination is abruptly truncated. Above the body the contact with unit F3 and its lowermost concretion beds are upwarped. Based on these features we interpret the conglomeratic body as the result of a shear zone.

Deposit G

Deposit G (Fig. 10) is composed of a sequence of chaotic breccias above scoured bases, and fining upwards sequences. It was observed relatively high up the mountain front, and the most easterly chaotic unit is interpreted as a debris flow in the proximal part of an alluvial fan, based on its scoured base and big blocks floating in a sandy matrix. The more westerly, distal part is interpreted as a stream flow unit, where gravels are well-sorted and imbricated, deposited on a channel-shaped erosional surface. No deformation was observed in this deposit.

5. Discussion

5.1. Quaternary evolution of Kyaukkyan Fault activity

There is abundant evidence of Quaternary deformation along the Kyaukkyan Fault.

In the Kyaukkyan and Indaw areas, to the north, stream offsets and deflections represent tangible evidence of strike-slip faulting, together with more recent superficial linear features observed north and south of the railway bend in Kyaukkyan village.

In the Inle Lake basin extensive alluvial fan sequences were deposited along the mountain front, indicating major activity in Quaternary to recent times. The alluvial fan sections at Nampan, near the southern end of Inle Lake, are characterised by dominant chaotic units with clear evidence of deformation that we interpret as the result of activity along the mountain front faults. The fan deposits are characterised by a lower deformed sequence separated by an erosional surface, that we name the 'prominent unconformity', from the overlying conglomeratic sequence that appears less deformed. Deformation of the lower sequence is expressed by a sharp fault contact of proximal-fan units with the bedrock, and faulting and folding of the mid- to distal-fan units. The uplifted hills on the Nampan alluvial fan system, south of Nampan, lie along the same N-S trend of the fold axis of these units, and the timing of deformation may be correlated between these deposits.

Dragged pebbles along a vertical fault contact between sediments and bedrock, in Deposit D, are the only evidence of deformation in the upper conglomeratic unit of the fan sequences. This could be related to reduction of recent fault activity at the basin margins.

Younger activity along the Kyaukkyan Fault is expressed not at the trnastensional basin's margins, but by clear evidence of deformation within the youngest, unconsolidated sediments of the basin centre (e.g. Figs. 3b, c; Fig. 13), corroborated by the offset of the Pawritha city wall north of Nyaungshwe (e.g. Soe Min et al., 2016). Preliminary

paleoseismologic trenching results confirm that historic fault activity occurred far from the prominent basin-bounding fault scarps (Crosetto et al*., In prep*).

Fig. 13 illustrates our interpretation of the fault system in the Inle Lake area. At Taunggyi the terraced topographic profile is an expression of basin-bounding normal faults dipping toward the centre of the basin; in the central part of the basin, N-S oriented ridges are interpreted as pressure ridges aligned along a N-S trending fault strand. Although locally transpressional, the cross-basin fault strand might be connected to the long-lived basin-bounding normal faults, forming a complex fault system. The through-going Kyaukkyan Fault itself, localised to the west by intra-basin uplift features, may be part of the same broad fault system (see inset of Fig. 13).

If we assume that these faults are upward splays of the same fault system, we can then infer the existence of a unique seismogenic source at depth that at different times has activated different fault segments at the surface, explaining the temporal change from deformation and neotectonic activity along the basin-bounding faults towards more recent cross-basin fault activity.

Alternatively, we can consider a progressive migration of fault activity towards a simple cross-basin strike-slip zone and abandonment of more complex sidewall normal fault systems, well documented from analogue models and known in literature as basin extinction (Zhang et al., 1989; Wu et al., 2009). There are abundant natural examples of the same process (e.g. Mann, 1997; Jaimes-Carvajal and Mann, 2003; Wu et al., 2009; Watkinson and Hall, 2017). If this evolutionary process has occurred, evidence of younger surface ruptures within the modern fluvial/lacustrine deposits of the Inle basin could be poorly preserved or rapidly lost due to surface processes and human activity. Perhaps this explains why evidence of historic events along the Kyaukkyan Fault, including the 1912 earthquake, remains so elusive.

5.2. The Kyaukkyan Fault and the 1912 Maymyo earthquake

Despite recent efforts to demonstrate a connection between the Kyaukkyan Fault and the 1912 Maymyo earthquake (Soe Min, 2010; Wang et al., 2014), it remains unclear whether that event originated on this fault or any other fault in in Central Myanmar. However, in this study we demonstrate conclusively that there has been Quaternary activity, including discrete surface rupturing paleoearthquakes along the fault. The continued lack of information about the fault's past seismic activity leaves an open question about whether the 1912 seismic event was unique or the last of a series of earthquakes with a long recurrence time.

The railway bend near Kyaukkyan village is the only physical evidence of potential surface deformation during the 1912 event (Coggin Brown, 1917; Wang et al., 2014; Soe Min et al., 2017). Our measurements along the railway, built in the late 19th Century and still in daily use, show a smooth deviation to the right of 2 ± 0.2 m, which may be interpreted as coseismic displacement. However, the pre-earthquake geometry of the railway is undocumented and the line may have originally featured an engineered curve. In the vicinity of the railway bend along the Kyaukkyan Fault scarp, decametric and potentially coseismic topographic elements in agricultural fields such as landforms representing uplift and subsidence lie along the same trend (Crosetto et al., 2016). These rather poorly constrained lines of evidence remain the only support for Kyaukkyan Fault rupture in 1912, making it pertinent to consider other seismic scenarios.

The historic identification of the Kyaukkyan Fault as the causative structure for the 1912 earthquake originated with Coggin Brown's survey of cultural damage in 1914, two years after the earthquake. Intense damage observed close to Kyaukkyan village defined a narrow zone along the Kyaukkyan Fault, resulting in mapped isoseismals with maximum intensity XI of the Rossi-Forel scale along the fault. At the time of the earthquake large tracts of Myanmar

were sparsely populated, resulting in a general lack of damage data over the Shan Plateau. It is possible that bias in contouring isoseismals along the (then) newly discovered Kyaukkyan Fault gave a false intensity distribution pattern that has influenced subsequent interpretations.

Perhaps the 1912 earthquake was actually relatively small in magnitude and not surface-rupturing, but caused disproportionate damage for its intensity. Such earthquakes are well documented in the historic record: the Bam, 2003 earthquake of M_w 6.5, and the Spitak, 1988 earthquake, of M_s 6.8, are two examples of moderate size events which caused destruction disproportionate to their size (e.g. Westaway, 1990; Hadjian, 1992), mainly caused by inappropriate construction design perhaps due to the absence of historical seismicity, leading to the collapse of more than 50% of the buildings (Talebian et al., 2004). Similarly, poorly designed construction, unusual ground conditions or slope instabilities might have amplified the destruction in the Kyaukkyan Fault area during the 1912 event, leading to an overestimation of its intensity.

5.2.1. 1912 rupture of the central/southern segment?

Alternatively, the 1912 failure of a southern segment of the Kyaukkyan Fault rather than the presumed northern segment could explain the absence of surface ruptures in the north. The tectonic geomorphology of the central and southern segments has been observed to be fresher than the northern segment (Soe Min, 2006; Wang et al., 2014; Soe Min et al., 2017). After the 1912 earthquake, the only reports of ground cracks (though likely gravity-related) were from the Inle Lake area (Soe Min, 2006). An example of probably young deformation of undated unconsolidated sediments was observed north of Taunggyi, as described in section 4.3.2. This subtle lineament parallel to the main topographic scarp may be the expression of surface rupture during a historic earthquake along the central/southern Kyaukkyan Fault, perhaps the 1912 event, despite a record of greater damage along the northern segment.

5.2.2. A non-Kyaukkyan Fault explanation for the 1912 event?

There are other potential seismic sources for the 1912 earthquake. Maymyo lies on the western Shan Plateau and is surrounded by active structures (e.g. Searle and Morley, 2011; Wang et al., 2014). The Sagaing Fault, to the west, is moving at 18-20 mm/yr (Vigny et al., 2003; Socquet et al., 2006), and has generated numerous destructive earthquakes recently and during the last century that may also have affected Maymyo (e.g. Hurukawa and Maung Maung, 2011; Wang et al. 2014). Indeed, in his report of the 1912 earthquake damage, Coggin-Brown (1917) stated that "*From a perusal of the detailed accounts of the damage in Mandalay* [40 km west of Maymyo/Pyin-Oo-Lwin and straddling the Sagaing Fault]*, it might be thought that the shock reached a higher intensity there than in Maymyo"*. Although his conclusion was that the Kyaukkyan Fault was more likely to be the source, the possibility of a previously unrecognised Sagaing Fault earthquake in 1912 cannot be eliminated.

Elsewhere, active E-W trending faults are widespread across the Shan Plateau near Pyin-Oo-Lwin, e.g. the Momeik Fault, Mae Chan Fault and Nam Ma Fault. Recent earthquakes on the Shan Plateau in eastern Myanmar include the M 6.8 Tarlay earthquake in 2011 on the Nam Ma Fault (e.g. Tun et al., 2014). GPS surveys are of poor spatial resolution and have been unable to clearly demonstrate whether residual India-Asia strain not taken up along the Sagaing Fault can be traced as far east as the Kyaukkyan Fault (e.g. Socquet et al., 2006).

Shan Plateau faults and deformation within the Myanmar Central Basin, conventionally attributed to northward motion of India, may also be influenced by or entirely driven by crustal flow around the Eastern Himalayan Syntaxis caused by gravitational collapse of the Tibetan Plateau (Rangin et al., 2013). It is clear that there are sufficient active structures and driving mechanisms in the region of Maymyo/Pyin-Oo-Lwin to provide numerous credible seismic sources for the 1912 earthquake, of which the Kyaukkyan Fault is just one.

6. Conclusions

- There is abundant evidence for Quaternary strike-slip displacement on the Kyaukkyan Fault, convincingly indicated by dextral stream offsets, deformed alluvial fans and intra-basin linear topographic features. Normal faulting along strike-slip basin margins is expressed by a low sinuosity mountain front onlapped by alluvial fan deposits that are locally faulted and folded.
- Ephemeral stream offsets with a statistical dextral peak of 125 m along the Gelaung valley are evidence of neotectonic strike-slip activity. Ephemeral streams, despite being of unknown age, are more likely to record only 'recent' deformation because of their ability to quickly re-straighten their courses, unlike offset deeply incised major rivers (e.g. Thanlwin river) which can preserve longer-term (pre-Quaternary?) offsets.
- There is limited evidence linking the 1912 earthquake to the Kyaukkyan Fault, and there are a number of alternative seismic scenarios:
  - Damage mapping in 1914 was conducted in non-urbanised areas and may have omitted significant coseismic surface deformation, leading to imprecise estimate of isoseismals;
  - The 1912 earthquake was smaller than M 8 and/or had limited surface expression but caused disproportionately large damage;
  - The 1912 earthquake ruptured the central/southern section of the Kyaukkyan Fault far from Maymyo;
  - Another fault such as the Sagaing Fault, rather than the Kyaukkyan Fault, was the seismic source of the 1912 event.
- A prominent unconformity marks the vertical transition from deformed alluvial fan sequences adjacent to bedrock basin margins, to overlying conglomerates that are undeformed or only weakly deformed. This unconformity might indicate that most recent strike-slip and transtensional activity has focused on more continuous pure strike-slip

fault segments along the axis of the basin rather than at the basin's margins, a migration process that is well known from natural examples of strike-slip basins and analogue models.

- The migration of fault activity towards a simple cross-basin strike-slip zone and the evidence of neotectonic activity along the Kyaukkyan Fault suggest that paleoseismic investigations should focus on more subtle cross-basin fault traces, far from the prominent, but less recently deformed mountain front scarps. Recommended future work includes palaeoseismological trenching across the cross-basin fault system in order to assess the magnitude and timing of past seismic events.

Acknowledgements

Robert Hall and an anonymous reviewer are thanked for their reviews which considerably improved this manuscript. We are grateful for substantial field assistance, logistical help and discussions in the field with Dr. Myo Thant, Dr. Lin Thu Aung and Myo Thu Soe; and for the valuable assistance of Mr Myint Naing during several field seasons. Funding for this research was provided by a RHUL Reid Scholarship, small grants from the RHUL Earth Sciences Research Committee and by the SE Asia Research Group at RHUL.

References

Abe, K., Noguchi, S.I., 1983. Revision of magnitudes of large shallow earthquakes, 1897-1912. Phys. Earth Planet. Inter. 33, 1–11.

Bertrand, G., Rangin, C., 2003. Tectonics of the western margin of the Shan plateau (central Myanmar): Implication for the India-Indochin oblique convergence since the Oligocene. J. Asian Earth Sci. 21, 1139–1157. doi:10.1016/S1367-9120(02)00187-6

Bertrand, G., Rangin, C., Maluski, H., Han, H., Thein, T.A., Myint, M., Maw, O., Lwin, S., 1999. Cenozoic metamorphism along the Shan scarp (Myanmar): evidences for ductile shear along the Sagaing Fault or the northward migration of the eastern Himalayan Syntaxis. Geophys. Res. Lett. 26, 915–918.

Blair, T.C., McPherson, J.G., 1994. Alluvial fans and their natural distinction from rivers based on morphology, hydraulic processes, sedimentary processes and facies assemblages. J. Sediment. Res. 3, 433–489.

Bowman, D., 1978. Determination of Intersection Points Within a Telescopic Alluvial Fan Complex. Earth Surf. Process. 3, 265–276. doi:10.1002/esp.3290030306

Burbank, D.W., Anderson, R.S., 2001. Tectonic Geomorphology. Blackwell publishing.

Burbank, D.W., Meigs, A.J., Brozović, N., 1996. Interactions of growing folds and coeval depositional systems. Basin Res. 8, 199–223. doi:10.1046/j.1365-2117.1996.00181.x

Chhibber, H.L., Ramamirtham, R., 1934. The geology of Burma. MacMillan, London.

Coggin Brown, J., 1917. The Burma Earthquake of May 1912: Mem. Geol. Surv. India 42, 1–147.

Corfield, R.I., Searle, M.P., 2000. Crustal shortening estimates across the north Indian

717 continental margin, Ladakh, NW India. Geol. Soc. London, Spec. Publ. 170, 395–410.

718 Crosetto, S., Watkinson, I.M., Gori, S., Falcucci, E., Soe Min, 2016. Tectonic geomorphology
719 and neotectonics of the Kyaukkyan Fault, Myanmar, in: EGU General Assembly
720 Conference Abstracts. p. 15322.

721 Curray, J.R., 2005. Tectonics and history of the Andaman Sea region. J. Asian Earth Sci. 25,
722 187–232. doi:10.1016/j.jseaes.2004.09.001

723 Curray, J.R., Moore, D.G., Lawver, L.A., Emmel, F.J., Raitt, R.W., Henry, M., Kieckhefer, R.,
724 1979. Tectonics of the Andaman Sea and Burma: convergent margins, in: Watkins, J.,
725 Montadert, L., Dickenson, P.W. (Eds.), Geological and Geophysical Investigations of
726 Continental Margins. American Association of Petroleum Geologists Special Volumes,
727 pp. 189–198.

728 Delcaillau, B., 2001. Geomorphic response to growing fault-related folds: example from the
729 foothills of central Taiwan. Geodin. Acta 14, 265–287. doi:10.1016/S0985-
730 3111(01)01071-3

731 Dooley, T., McClay, K., 1997. Analogue modelling of pull-apart basins. Am. Assoc. Pet. Geol.
732 Bull. 81, 1804–1826.

733 Fu, B., Awata, Y., Du, J., He, W., 2005. Late Quaternary systematic stream offsets caused by
734 repeated large seismic events along the Kunlun fault, northern Tibet. Geomorphology
735 71, 278–292. doi:http://dx.doi.org/10.1016/j.geomorph.2005.03.001

736 Galadini, F., Falcucci, E., Galli, P., Giaccio, B., Gori, S., Messina, P., Moro, M., Saroli, M.,
737 Scardia, G., Sposato, A., 2012. Time intervals to assess active and capable faults for
738 engineering practices in Italy. Eng. Geol. 139–140, 50–65.
739 doi:10.1016/j.enggeo.2012.03.012

740 Gutenberg, B., Richter, C.F., 1996. Magnitude and Energy of Earthquakes. Ann. Geofis. 1–15.

741 Hadjian, A.H., 1992. The Spitak, Armenia earthquake - Why so much destruction?, in:
742 Earthquake Engineering, Tenth World Conference. Balkema, Rotterdam.

743 Hall, R., 2012. Late Jurassic-Cenozoic reconstructions of the Indonesian region and the Indian
744 Ocean. Tectonophysics 570–571, 1–41. doi:10.1016/j.tecto.2012.04.021

745 Hall, R., 2002. Cenozoic geological and plate tectonic evolution of SE Asia and the SW Pacific:
746 computer-based reconstructions, model and animations. J. Asian Earth Sci. 20, 353–
747 434.

748 Hall, R., van Hattum, M.W.A., Spakman, W., 2008. Impact of India–Asia collision on SE Asia:
749 the record in Borneo. Tectonophysics 451, 366–389.

750 Harvey, A.M., Mather, A.E., Stokes, M., 2005. Alluvial fans: geomorphology, sedimentology,
751 dynamics—introduction. A review of alluvial-fan research., in: Harvey, A.M., Mather,
752 A.E., Stokes, M. (Eds.), Alluvial Fans: Geomorphology, Sedimentology, Dynamics.
753 Geological Society of London Special Publication, 251, London, pp. 1–7.

754 Holt, W.E., Ni, J.F., Wallace, T.C., Haines, A.J., 1991. The active tectonics of the Eastern
755 Himalayan Syntaxis and surrounding regions. J. Geophys. Res. 96, 14595–14632.
756 doi:10.1029/91JB01021

757 Hurukawa, N., Maung Maung, P., 2011. Two seismic gaps on the Sagaing Fault, Myanmar,
758 derived from relocation of historical earthquakes since 1918. Geophys. Res. Lett. 38.

759 Jaimes-Carvajal, M., Mann, P., 2003. Tectonic origin of the Cariaco basin, Venezuela: Pull-
760 apart, extinct pull-apart, or fault-normal extension, in: AAPG Annual Meeting, Salt Lake
761 City, Utah.

762 Kleinhans, M.G., Markies, H., De Vet, S.J., Veld, A.C., Postema, F.N., 2011. Static and dynamic

763 angles of repose in loose granular materials under reduced gravity. J. Geophys. Res. E
764 Planets 116, 1–13. doi:10.1029/2011JE003865

765 La Touche, T.H.D., 1913. Geology of the northern Shan States. Office of the Geological survey.

766 Lacassin, R., Leloup, P.H., Tapponnier, P., 1993. Bounds on strain in large Tertiary shear zones
767 of SE Asia from boudinage restoration. J. Struct. Geol. 15, 677–692.

768 Lacassin, R., Maluski, H., Leloup, P.H., Tapponnier, P., Hinthong, C., Siiribhakdi, K., Chuaviroj,
769 S., Charoenravat, A., 1997. Tertiary diachronic extrusion and deformation of western
770 Indochina: Structural and 40Ar/39Ar evidence from NW Thailand. J. Geophys. Res. 102,
771 10,013-10,037.

772 Lacassin, R., Replumaz, A., Leloup, P.H., 1998. Hairpin river loops and slip-sense inversion' on
773 southeast Asian strike-slip faults. Geology 26, 703–706. doi:10.1130/0091-
774 7613(1998)026<0703:HRLASS>2.3.CO;2

775 Le Dain, A.Y., Tapponnier, P., Molnar, P., 1984. Active faulting and tectonics of Burma and
776 surrounding regions. J. Geophys. Res. 89, 453–472.

777 Lee, T.-Y., Lawver, L.A., 1995. Cenozoic plate reconstruction of Southeast Asia.
778 Tectonophysics 251, 85–138.

779 Machette, M.N., 2000. Active, capable, and potentially active faults - a paleoseismic
780 perspective. J. Geodyn. 29, 387–392. doi:10.1016/S0264-3707(99)00060-5

781 Mann, P., 1997. Model for the formation of large, transtensional basins in zones of tectonic
782 escape. Geology 25, 211–214.

783 Mitchell, A.H.G., 1993. Cretaceous-Cenozoic tectonic events in the western Myanmar
784 (Burma)-Assam region. J. Geol. Soc. London. 150, 1089–1102.
785 doi:10.1144/gsjgs.150.6.1089

786 Mitchell, A.H.G., Hlaing, T., Nyunt Htay, 2002. Mesozoic orogenies along the Mandalay-
787 Yangon margin of the Shan Plateau, in: Montajit, N. (Ed.), Symposium on the Geology
788 of Thailand. Bangkok, pp. 136–149.

789 Mitchell, A.H.G., Myint Thein Htay, Kyaw Min Htun, Myint Naing Win, Thura Oo, Tin Hlaing,
790 2007. Rock relationships in the Mogok metamorphic belt, Tatkon to Mandalay, central
791 Myanmar. J. Asian Earth Sci. 29, 891–910. doi:10.1016/j.jseaes.2006.05.009

792 Mitchell, A.H.G., Sun-lin Chung, Thura Oo, Te-hsien Lin, Chien-hui Hung, 2012. Zircon U – Pb
793 ages in Myanmar : Magmatic – metamorphic events and the closure of a neo-Tethys
794 ocean ? J. Asian Earth Sci. 56, 1–23. doi:10.1016/j.jseaes.2012.04.019

795 Mohadjer, S., Bendick, R., Ischuk, A., Kuzikov, S., Kostuk, A., Saydullaev, U., Lodi, S., Kakar,
796 D.M., Wasy, A., Khan, M.A., Molnar, P., Bilham, R., Zubovich, A.V., 2010. Partitioning of
797 India-Eurasia convergence in the Pamir-Hindu Kush from GPS measurements. Geophys.
798 Res. Lett. Res. Lett. 37. doi:http://dx.doi.org/10.1029/2009GL041737

799 Molnar, P., Tapponnier, P., 1975. Cenozoic tectonics of Asia effects of a continental collision.
800 Science (80-.). 189, 419–426.

801 Morley, C.K., 2013. Discussion of tectonic models for Cenozoic strike-slip fault-affected
802 continental margins of mainland SE Asia. J. Asian Earth Sci. 76, 137–151.

803 Morley, C.K., 2009. Evolution from an oblique subduction back-arc mobile belt to a highly
804 oblique collisional margin: the Cenozoic tectonic development of Thailand and eastern
805 Myanmar. Geol. Soc. London, Spec. Publ. 318, 373–403. doi:10.1144/SP318.14

806 Morley, C.K., 2004. Nested strike-slip duplexes, and other evidence for Late Cretaceous-
807 Palaeogene transpressional tectonics before and during India-Eurasia collision, in
808 Thailand, Myanmar and Malaysia. J. Geol. Soc. London. 161, 799–812.

809 Morley, C.K., Smith, M., Carter, A., Charusiri, P., Chantraprasert, S., 2007. Evolution of
810 deformation styles at a major restraining bend, constraints from cooling histories, Mae
811 Ping Fault Zone, Western Thailand, in: Cunningham, W.D., Mann, P. (Eds.), Tectonics of
812 Strike-Slip Restraining and Releasing Bends. Geological Society, Special Publications,
813 London, pp. 325–349.

814 Ngwe Sint, U., Catalan, I., 2000. Preliminary survey on potentiality of reforestation under
815 clean development mechanism in Myanmar with particular reference to Inle region.
816 Unpubl. Rep. by Karamosia Intl., Yangoon.

817 Nichols, G., 2009. Sedimentology and stratigraphy, 2nd ed. Wiley-Blackwell, Chichester.

818 Pacheco, J.F., Sykes, L.R., 1992. Seismic moment catalogue of large shallow earthquakes,
819 1900 to 1989. Bull. Seismol. Soc. Am. 82, 1306–1349.

820 Pope, R.J.J., Wilkinson, K.N., 2005. Reconciling the roles of climate and tectonics in Late
821 Quaternary fan development on the Spartan piedmont, Greece, in: Harvey, A.M.,
822 Mather, A.E., Stokes, M. (Eds.), Alluvial Fans: Geomorphology, Sedimentology,
823 Dynamics. Geological Society of London Special Publication, 251, pp. 133–152.

824 Rangin, C., Maurin, T., Masson, F., 2013. Combined effects of Eurasia/Sunda oblique
825 convergence and East-Tibetan crustal flow on the active tectonics of Burma. J. Asian
826 Earth Sci. 76, 185–194.

827 Reading, H.G. (editor), 2009. Sedimentary environments; processes, facies and stratigraphy,
828 3rd ed. Wiley-Blackwell, Oxford, UK.

829 Replumaz, A., Lacassin, R., Tapponnier, P., Leloup, P.H., 2001. Large river offsets and Plio-
830 Quaternary dextral slip rate on the Red River fault (Yunnan, China). J. Geophys. Res.
831 106, 819–836.

832 Ridd, M.F., Watkinson, I., 2013. The Phuket-Slate Belt terrane: tectonic evolution and strike-
833 slip emplacement of a major terrane on the Sundaland margin of Thailand and
834 Myanmar. Proc. Geol. Assoc. 124, 994–1010. doi:10.1016/j.pgeola.2013.01.007

835 Sahu, V.K., Gahalaut, V.K., Rajput, S., Chadha, R.K., Laishram, S.S., Kumar, A., 2006. Crustal
836 deformation in the Indo-Burmese arc region: Implications from the Myanmar and
837 Southeast Asia GPS measurements. Curr. Sci. 90, 1688–1693.

838 Searle, D.L., Haq, B.T., 1964. The Mogok Belt of Burma and its relationship to the Himalayan
839 Orogeny. Proc. Int. Geol. Congr. 22, 132–161.

840 Searle, M.P., Morley, C.K., 2011. Tectonics and thermal evolution of Thailand in the regional
841 context of Southeast Asia, in: Ridd, M.F., Barber, A.J., Crow, M.J. (Eds.), The Geology of
842 Thailand. Geological Society, London, pp. 539–572.

843 Searle, M.P., Noble, S.R., Cottle, J.M., Waters, D.J., Mitchell, A.H.G., Hlaing, T., Horstwood,
844 M.S. a, 2007. Tectonic evolution of the Mogok metamorphic belt, Burma (Myanmar)
845 constrained by U-Th-Pb dating of metamorphic and magmatic rocks. Tectonics 26, n/a-
846 n/a. doi:10.1029/2006TC002083

847 Shen, Z.K., Lü, J., Wang, M., Bürgmann, R., 2005. Contemporary crustal deformation around
848 the southeast borderland of the Tibetan Plateau. J. Geophys. Res. Solid Earth 110, 1–
849 17. doi:10.1029/2004JB003421

850 Sidle, R.C., Ziegler, A.D., Vogler, J.B., 2007. Contemporary changes in open water surface area
851 of Lake Inle, Myanmar. Sustain. Sci. 2, 55–65. doi:10.1007/s11625-006-0020-7

852 Socquet, A., Pubellier, M., 2005. Cenozoic deformation in western Yunnan (China-Myanmar
853 border). J. Asian Earth Sci. 24, 495–515. doi:10.1016/j.jseaes.2004.03.006

854 Socquet, A., Vigny, C., Chamot-Rooke, N., Simons, W., Rangin, C., Ambrosius, B., 2006. India

855 and Sunda plates motion and deformation along their boundary in Myanmar
856 determined by GPS. J. Geophys. Res. Solid Earth 111, 1–11.

857 Soe Min, 2010. Structural study along the Kyaukkyan Fault, Shan State. University of Yangon.

858 Soe Min, 2006. Urban geology of Taunggyi and Ayethayar. Taunggyi University, Myanmar.

859 Soe Min, Watkinson, I.M., Soe Thura Tun, Win Naing, 2017. The Kyaukkyan Fault, in: Barber,
860 A. J., Khin Zaw & Crow, M. J. (eds). Myanmar: Geology, Resources and Tectonics. Geol.
861 Soc., London, Mem., 48, 453–471, https://doi.org/10.1144/M48.21

862 Soe Thura Tun, Wang, Y., Saw Ngwe Khaing, Myo Thant, Nyunt Htay, Yin Myo Min Htwe, Than
863 Myint, Sieh, K., 2014. Surface Ruptures of the Mw 6.8 March 2011 Tarlay Earthquake,
864 Eastern Myanmar. Bullettin Seismol. Soc. Am. 104, 2915–2932.
865 doi:10.1785/0120130321.

866 Soe Thura Tun, Watkinson, I.M., 2017. The Sagaing Fault, in: in: Barber, A. J., Khin Zaw &
867 Crow, M. J. (eds). Myanmar: Geology, Resources and Tectonics. Geol. Soc., London,
868 Mem., 48, 413–441, https://doi.org/10.1144/M48.19.

869 Sone, M., Metcalfe, I., 2008. Parallel Tethyan sutures in mainland Southeast Asia: new
870 insights for Palaeo-Tethys closure and implications for the Indosinian orogeny. C.R.
871 Geosci. 340, 166‑179.

872 Talebian, M., Fielding, E.J., Funning, G.J., Ghorashi, M., Jackson, J., Nazari, H., Parsons, B.,
873 Priestley, K., Rosen, P.A., Walker, R., Wright, T.J., 2004. The 2003 Bam (Iran) earthquake:
874 Rupture of a blind strike-slip fault. Geophys. Res. Lett. 31, n/a-n/a.
875 doi:10.1029/2004GL020058

876 Tapponnier, P., Peltzer, G., Le Dain, A.Y., Armijo, R., Cobbold, P.R., 1982. Propagating
877 extrusion tectonics in Asia: New insights from simple experiments with plasticine.

878 Geology 10, 611–616.

879 Timm, T., Arslan, N., Rüzgar, M., Martinsson, S., Erséus, C., 2013. Oligochaeta (Annelida) of
880 the profundal of Lake Hazar (Turkey), with description of Potamothrix alatus hazaricus
881 n. ssp. Zootaxa 3716, 144–156. doi:10.11646/zootaxa.3716.2.2.

882 Vigny, C., Socquet, A., Rangin, C., Chamot-Rooke, N., Pubellier, M., Bouin, M., Bertrand, G.,
883 Becker, M., 2003. Present-day crustal deformation around Sagaing fault, Myanmar. J.
884 Geophys. Res. Solid Earth 108.

885 Wallace, R.E., 1968. Notes on stream channels offset by the San Andreas fault, southern
886 Coast Ranges, California. Dickinson, W.R., Grantz, A. (Eds.), Conf. Geol. Probl. San
887 Andreas Fault Syst. Stanford Univ. Publ. Geol. Sci. 11, 6–21.

888 Wang, E., Burchfiel, B.C., Royden, L.H., Chen, L., Chen, J., Li, W., Chen, Z., 1998. Late Cenozoic
889 Xianshuihe-Xiaojiang, Red River, and Dali Fault Systems of Southwestern Sichuan and
890 Central Yunnan, China, in: Special Paper 327: Late Cenozoic Xianshuihe-Xiaojiang, Red
891 River, and Dali Fault Systems of Southwestern Sichuan and Central Yunnan, China.
892 Geological Society of America, pp. 1–108. doi:10.1130/0-8137-2327-2.1.

893 Wang, J., Peng, P., Ma, Q., Zhu, L., 2013. Investigation of water depth,water quality and
894 modern sedimentation rate in Mapam Yumco and La'ang Co,Tibet. J. lake Sci. 4.

895 Wang, Y., Sieh, K., Soe Min, Khaing, S., Tun, S.T., 2009. Smoking gun of the May-1912 Burma
896 earthquake? Neotectonics of the Kyaukkyan fault system, Eastern Burma (Myanmar),
897 in: AGU. San Francisco, California.

898 Wang, Y., Sieh, K., Soe Thura Tun, Kuang Yin Lai, Than Myint, 2014. Active tectonics and
899 earthquake potential of the Myanmar region. J. Geophys. Res. Solid Earth 119, 3767–
900 3822. doi:10.1002/2013JB010762

Watkinson, I.M., Hall, R., 2017. Fault systems of the eastern Indonesian triple junction: evaluation of Quaternary activity and implications for seismic hazards, in: Cummins, P.R., Meilano, I. (Eds.), Geohazards in Indonesia: Earth Science for Disaster Risk Reduction. Geological Society of London, Special Publicantions, 441, 71–120. doi:10.1144/SP441.8.

Westaway, R., 1990. Seismicity and tectonic deformation rate in Soviet Armenia: implications for local earthquake hazard and evolution of adjacent regions. Tectonics 9, 477–503.

Win Swe, 2012. Outline geology and economic mineral occurrences of the union of Myanmar. J. Myanmar Geosciences Soc., Special Publication, 1, 1–136.

Wu, J.E., McClay, K., Whitehouse, P., Dooley, T., 2009. 4D analogue modelling of transtensional pull-apart basins. Mar. Pet. Geol. 26, 1608–1623. doi:10.1016/j.marpetgeo.2008.06.007

Yin, A., Harrison, T.M., 2000. Geologic evolution of the Himalayan-Tibetan orogen. Annu. Rev. Earth Planet. Sci. 28, 211–280.

Zhang, P., Burchfiel, B.C., Chen, S., Deng, Q., 1989. Extinction of pull-apart basins. Geology 17, 814–817.

Figure captions

Fig. 1: Kyaukkyan Fault location and overview, with a Shuttle Radar Topography (SRTM) 90 m base DEM. a) Tectonic setting of the Kyaukkyan Fault. Sibumasu terrane shaded in yellow. Modified after Soe Min et al., 2017. b), c) Main faults and lineaments along the northern (a) and southern (b) Kyaukkyan fault system; map locations shown in Fig. 1a. *NP*: Nawnghkio Plateau; *KP*: Kyaukku Plateau.

Fig. 2: Schematic representation of the observed geologic and geomorphic features associated with Quaternary to recent activity along the Kyaukkyan Fault. a) Inherited offset and deflection of geomorphic markers along a basin-bounding fault (A) and younger offset of markers including man-made structures and self-healing rivers along an active intra-basin fault (B); b) planar fault scarp with triangular facets; c) sealed basin-bounding fault, superseded by an upward splay in the hanging wall. Recent activity is indicated by sand ejection along the fault trace within basinal lacustrine sediments; d) wind gap developed in a deformed range-front alluvial fan; e) partly buried fault contact between bedrock and syn-tectonic alluvial fan.

Fig. 3: The Mandalay-Lashio metre-gauge railway at Kyaukkyan village, showing 2.0 ± 0.2 m apparent dextral offset of the tracks just east of an inactive bedrock fault scarp. View to west.

Fig. 4: Stream offset restoration along the basin-bounding fault system at Gelaung valley. a) Panoramic view to the east of the Gelaung valley range front scarp, showing geomorphic features including offset streams and shutter ridges; two fault strands are indicated by the short arrows. b) Topographic map of Nawnghkio Plateau scarp with ephemeral streams (blue lines) and Kyaukkyan Fault trace used in the recovery (red line). Note that the map is rotated so north is to the left. c) Recovery of ephemeral streams. Light blue, dashed lines represent modern stream pattern; dark blue lines represent the recovered stream pattern. d), e) Histograms showing the distribution of number of streams (y axis) for incremental

restoration displacement (x axis) restored by shifting to the left the block to the east of the fault trace. d) represents the quantitative distribution for offset increments of 25 m, up to 1600 m of restoration; e) represents a qualitative restoration of selected deflected streams. Map location shown in Fig. 1b.

Fig. 5: Kyaukkyan Fault trace (red dashed lines) at Zawgyi reservoir. White dotted lines represent rivers. a) Overview of the Zawgyi reservoir area. Base map from ESRI World Imagery compilation, which includes <1 m DigitalGlobe imagery. b) Satellite image with detail of deflected rivers (white dotted lines) and trace of the paleoriver (white dashed lines) (Google Earth 2014). Arrows indicate river flow direction. c) Offset and beheaded dry stream south of Zawgyi reservoir. Figure location shown in Fig. 1b.

Fig. 6: Inle basin map showing topography, key Quaternary deposits and structural elements. a) Inle Lake area. b) Mobye dam area, south of Inle Lake. Map locations shown in Fig. 1c.

Fig. 7: a) Modern watercourse of the Thanlwin river across the Kyaukkyan Fault at the Thai-Myanmar border; and b) restoration of 2.3 ± 0.2 km dextral offset along the main strand of the Kyaukkyan Fault. Map locations shown in Fig. 1a.

Fig. 8: a) Google Earth image of a linear pale trace, corresponding to the fault trace, in unconsolidated sediments close to the bedrock contact in the northern Inle basin. Note that north is to the left; the eye indicates the view of b); white arrows locate the fault trace. b) Field photo, view to SW showing the subtle topographic scarp and linear pale trace within unconsolidated sediments.

Fig. 9: a) Google Earth image showing alluvial fans burying and being deformed by the basin bounding fault system on the east side of the Inle basin at Nampan. b) Interpretation highlighting the relationship between: the alluvial fans; the uplifted hills SE of Nampan directly along strike from the folded unit in Deposit F of Nampan quarry to the north ('X'

symbol, and quarry roads shown by dot-dashed lines); the paleo-river deflected as a consequence of the hills' uplift and the resultant water gap; the topographic scarp developed on the fans (see also Fig. 2d). c) Schematic evolution of the alluvial fan system during five sequential time stages. Uplift: '+'; subsidence: '-'. Map location shown in Fig. 6.

Fig. 10: 2004 Google Earth image of the eastern Inle basin mountain front, with location of sedimentary logs relative to Nampan quarry alluvial deposits that bury the basin bounding fault trace approximately on the topographic scarp. Note the image is rotated so north is to the left. The red line in all sedimentary logs represents the prominent unconformity. Stars indicate the location of pictures in Fig. 12; dashed white lines represent the quarry's roads. For sedimentary facies descriptions and other details see text. Map location shown in Fig. 6.

Fig. 11: a) Sub-vertical bedding in low grade metasedimentary basement below the alluvial fan successions exposed in Nampan quarry. b) Catastrophic flow facies of Deposit A. c) Sheet flow facies of Deposit E. d) Chaotic conglomeratic body laterally truncating the gravel layers in Deposit F. All photos show sub-vertical man-made road sections. Photo location and relative stratigraphic positions are shown in logs of Fig. 10.

Fig. 12: Field photos and interpretation of deformed alluvial fan deposits of Nampan quarry site. All photos show sub-vertical man-made road sections. Interpretation drawings: red dashed lines represent fault zones (b, c, h) or fault lines (f); Ch: channel; C_S: stratified conglomerate; C_M: massive conglomerate; S_S: stratified sandstone; S_M: massive sandstone; B: bedrock. a), b) Steeply-dipping sediments of Deposit A. c), d) Fault in lower units sealed by upper deposits lying above prominent unconformity in Deposit C. e), f) Gravel-filled channel cut by fault and showing apparent vertical displacement in Deposit D. g), h) Fault drag of clasts and weathered bedrock at the bedrock/alluvial fan interface in Deposit D. The blue dashed line indicates the progressive rotation of the long axes of dragged clasts. i), j) Gentle folding of syn-tectonic alluvial sediments and truncation by the prominent unconformity in

992 Deposit F; on the right shaded in grey, a body of chaotic conglomerate laterally truncates the
993 gravel layers (see Fig. 11d). Photo locations shown in Fig. 10.

994 **Fig. 13:** Serial cross-sections of the basin-bounding fault system at the eastern margin of Inle
995 basin (topographic profiles derived from ASTER 30 m GDEM, x2.5 vertical exaggeration).
996 Interpreted faults are linked to schematically represent the 3D fault system as it converges
997 into a single strand in the south and possibly at depth. Inset shows the location of profiles
998 and map view, and highlights the relationship between the basin bounding fault system and
999 the main cross-basin Kyaukkyan Fault strand further west. Map location of profiles is shown
1000 in Fig. 6.

Fig. 1

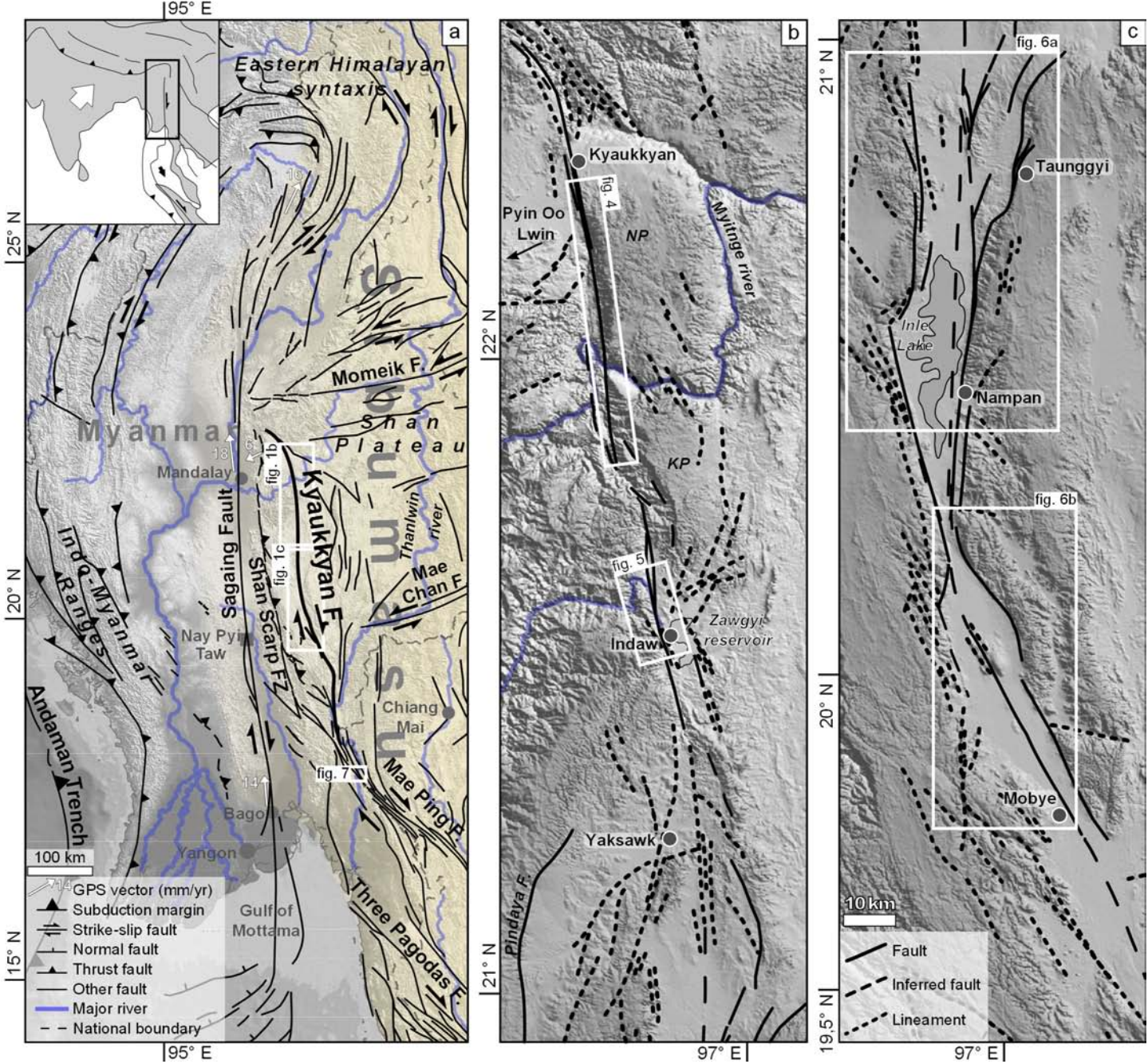
a
b
c
95° E
25° N
20° N
15° N
Eastern Himalayan syntaxis
Myanmar
Shan Plateau
Momeik F.
Mandalay
Sagaing Fault
Kyaukkyan F.
Shan Scarp FZ
Nay Pyi Taw
Indo-Myanmar Ranges
Andaman Trench
Thanlwin river
Mae Chan F.
Chiang Mai
Mae Ping F.
Three Pagodas F.
Bago
Yangon
Gulf of Mottama
Sunda
fig. 1b
fig. 1c
fig. 7
100 km
GPS vector (mm/yr)
Subduction margin
Strike-slip fault
Normal fault
Thrust fault
Other fault
Major river
National boundary
Kyaukkyan
Pyin Oo Lwin
fig. 4
NP
Myitnge river
KP
fig. 5
Indaw
Zawgyi reservoir
Yaksawk
Pindaya F.
21° N
22° N
97° E
fig. 6a
Taunggyi
Inle Lake
Nampan
fig. 6b
Mobye
10 km
Fault
Inferred fault
Lineament
19,5° N
21° N
20° N
97° E

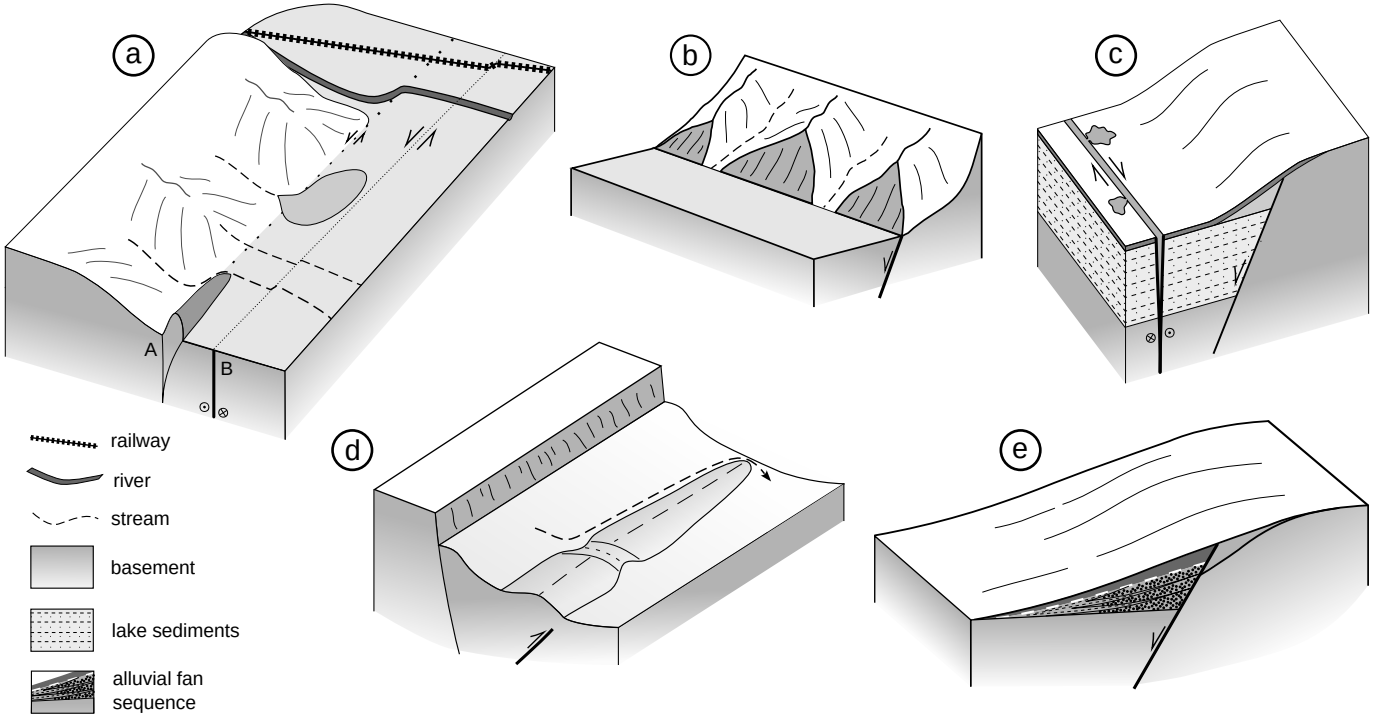
a
b
c
d
e
A
B
railway
river
stream
basement
lake sediments
alluvial fan
sequence

Fig. 2

Fig. 3

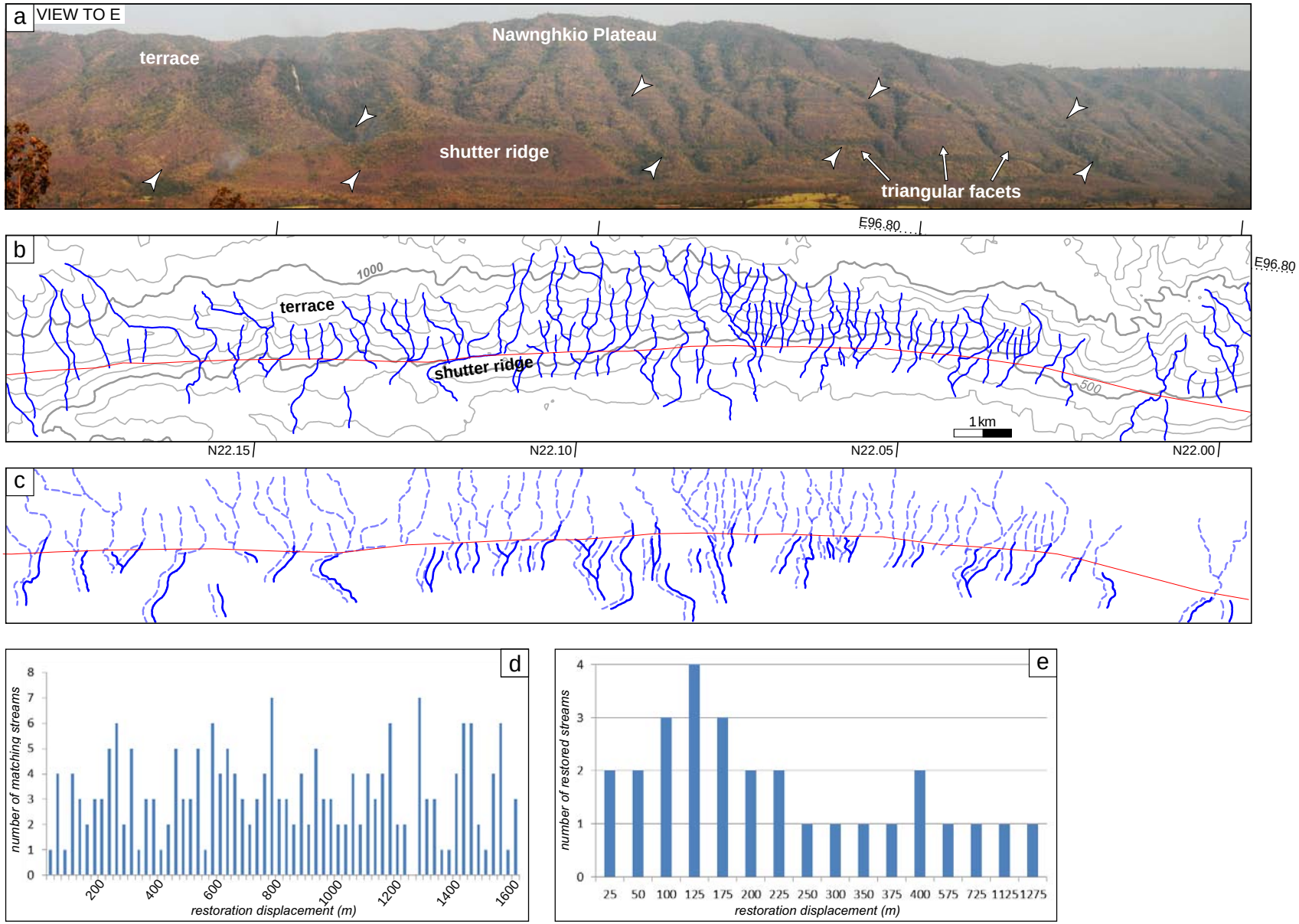
a
VIEW TO E
Nawnghkio Plateau
terrace
shutter ridge
triangular facets
b
E96.80
E96.80
1000
terrace
shutter ridge
500
1 km
N22.15
N22.10
N22.05
N22.00
c
d
number of matching streams
0
1
2
3
4
5
6
7
8
200
400
600
800
1000
1200
1400
1600
restoration displacement (m)
e
number of restored streams
0
1
2
3
4
25
50
100
125
175
200
225
250
300
350
375
400
575
725
1125
1275
restoration displacement (m)

Fig. 4

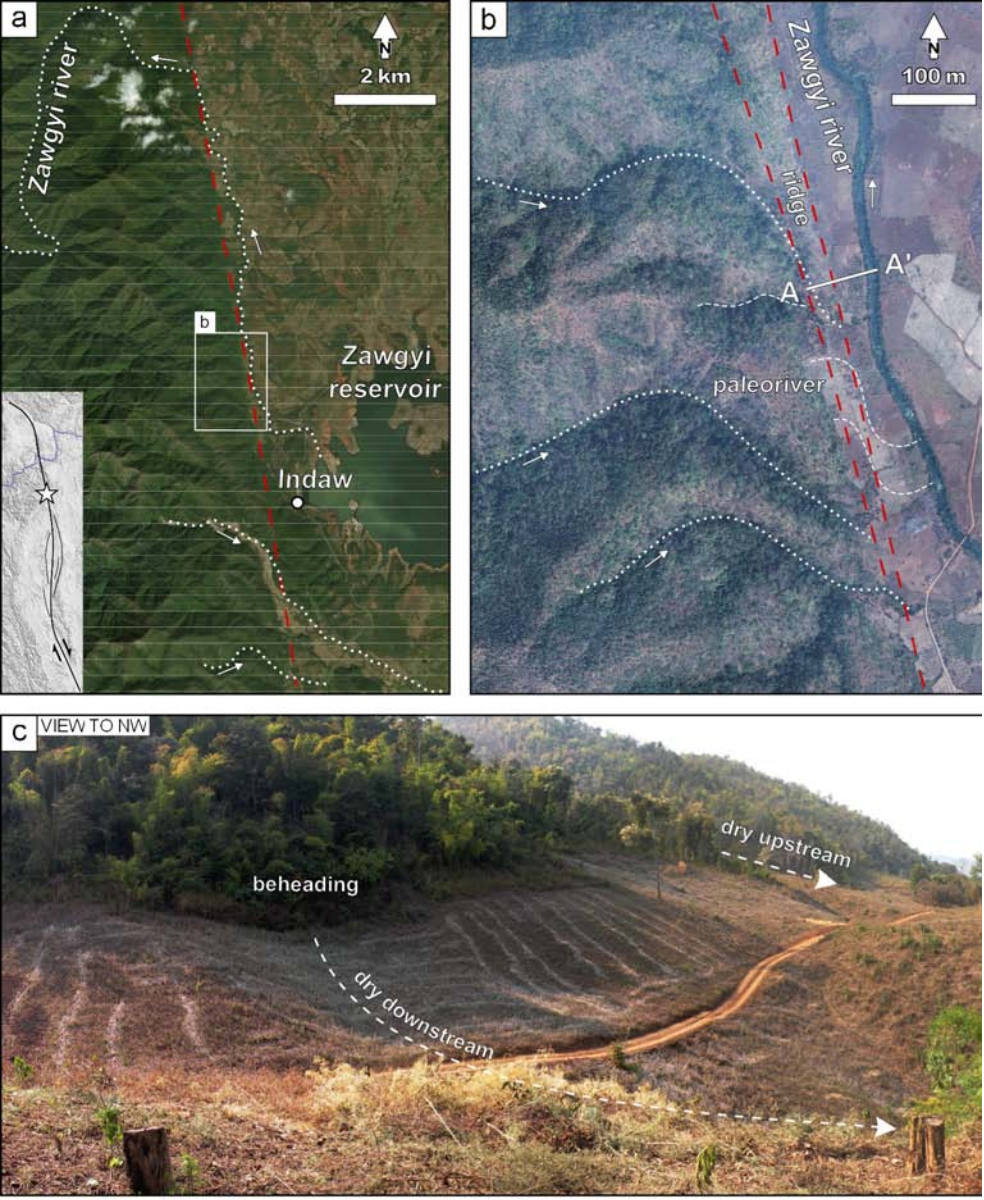
a
N
2 km
Zawgyi river
b
Zawgyi
reservoir
Indaw
b
Zawgyi river
N
100 m
ridge
A
A'
paleoriver
c
VIEW TO NW
dry upstream
beheading
dry downstream

Fig. 5

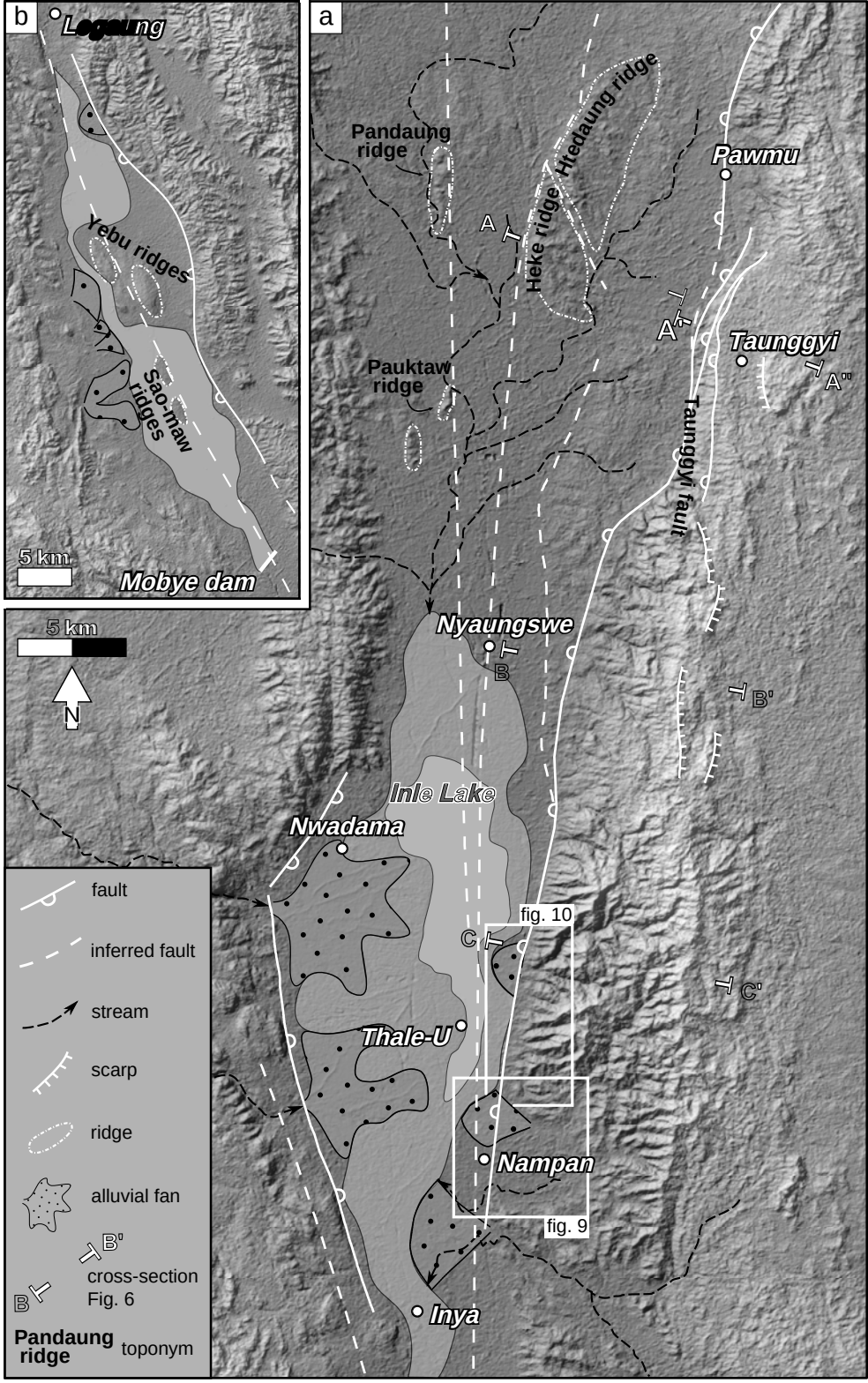
b
Loggaung
Yebu ridges
Sao-maw ridges
5 km
Mobye dam
a
Pandaung ridge
Hiedaung ridge
Heke ridge
Pawmu
A
A'
Taunggyi
A"
Pauktaw ridge
Taunggyi fault
Nyaungswe
B
B'
5 km
N
Inle Lake
Nwadama
fig. 10
C
C'
Thale-U
Nampan
fig. 9
Inya
fault
inferred fault
stream
scarp
ridge
alluvial fan
B'
cross-section
Fig. 6
B
Pandaung ridge
toponym

Fig.6

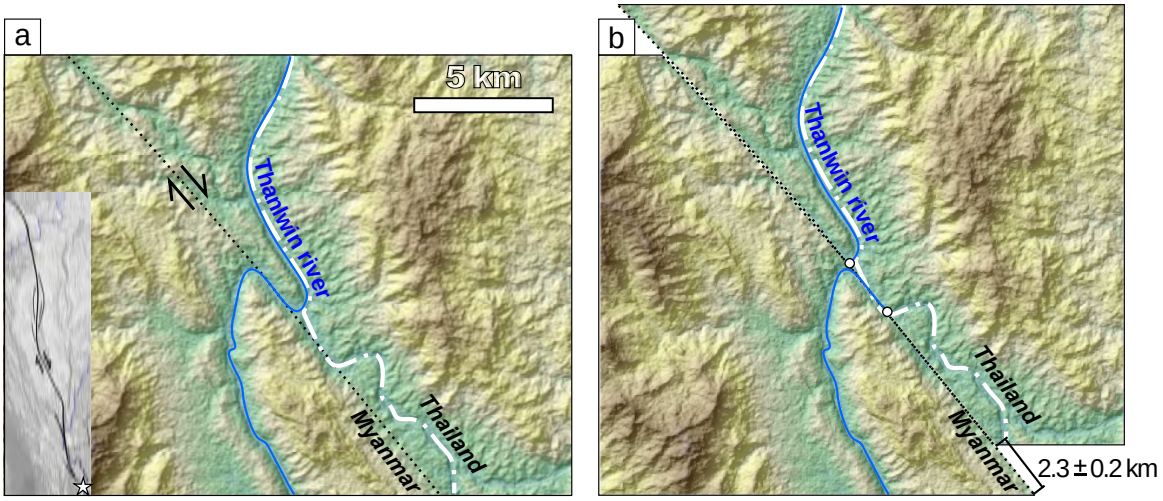
a
5 km
Thanlwin river
Thailand
Myanmar
b
Thanlwin river
Thailand
Myanmar
2.3 ± 0.2 km

Fig. 7

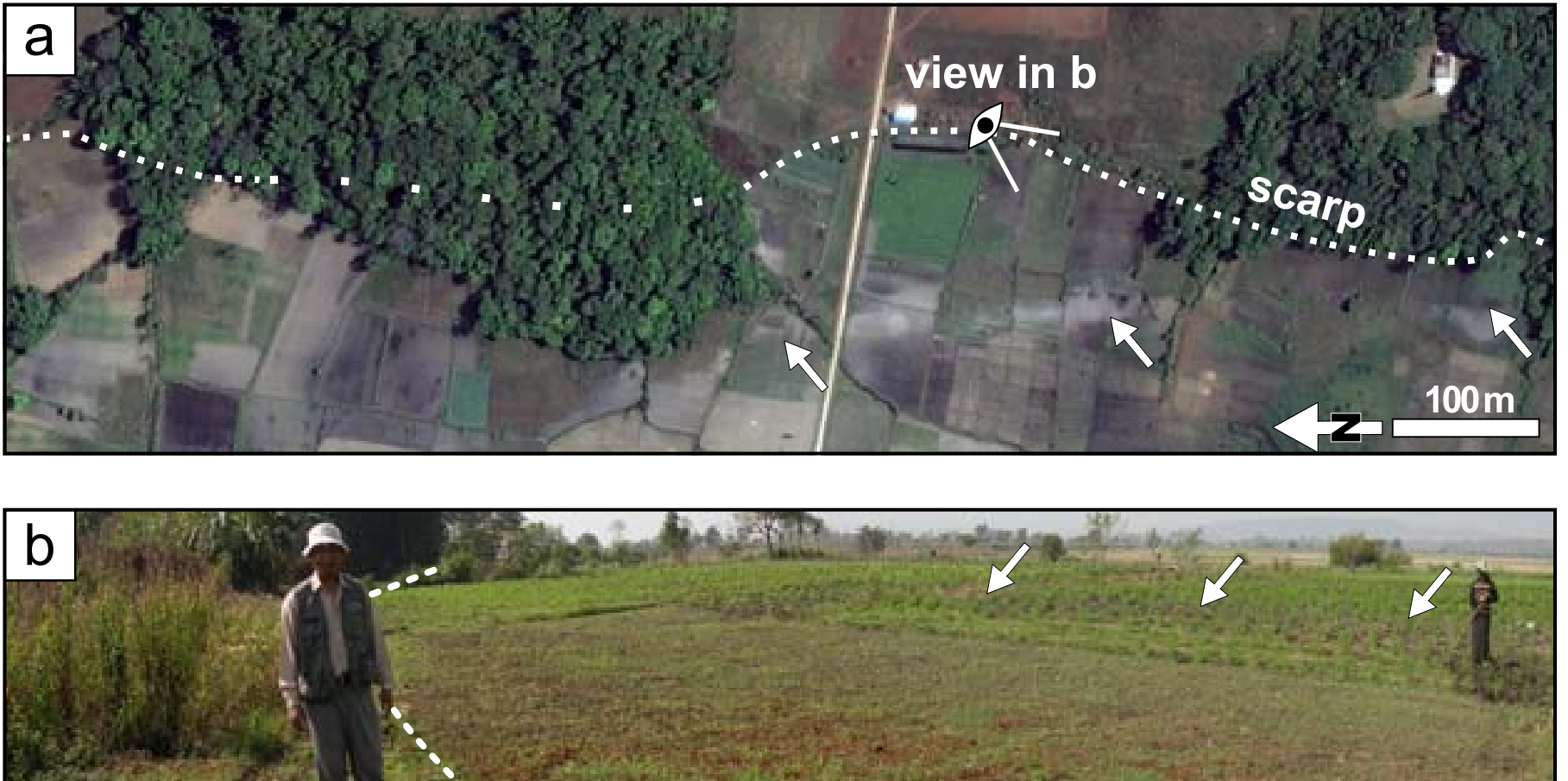

Fig. 8

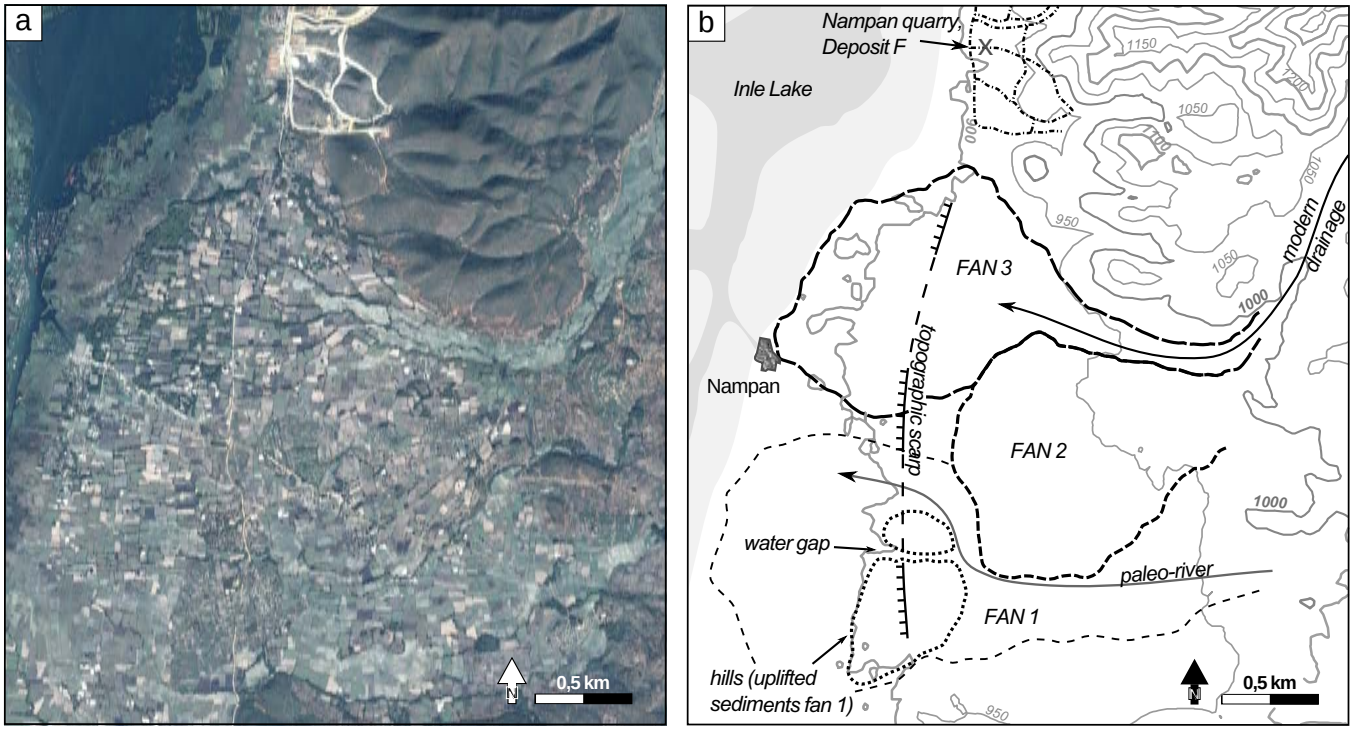

I. *The depocentre of the basin is in the S; alluvial fan 1 is deposited by stream A.*

II. *The S part of the basin experiences compression, and starts to uplift.*

III. *The folded deposits of fan 1 are uplifted and eroded by stream A that creates a water-gap. Alluvial fan 2 is being deposited by stream B.*

IV. *The uplift of the hills on fan 1 causes deviation of stream A, and fan 1 becomes inactive. The uplift of the southern area causes northwards shift of stream B.*

V. *A new alluvial fan 3 is formed by stream B, and fan 2 becomes inactive.*

Fig. 8


A Distal
m | s | sand | grav
1m
1.3 m
1m
Fig.11b
A Proximal
m | s | sand | grav
< 2 m
SSW
B
m | s | sand | grav
1.5 m
1.5 m
0.5 m
1m
E
m | s | sand | grav
3 m
Fig.11c
G
m | s | sand | grav
1.7 m
2 m
0.5 m
W
N
500 m
Fig.12a
Fig.12c
Fig.12e, g
Fig.12i
C Proximal
m | s | sand | grav
< 2 m
C Mid
m | s | sand | grav
1m
1m
1m
1m
W
C Distal
m | s | sand | grav
1m
1.5 m
1m
1m
WSW/S
D Proximal
m | s | sand | grav
1m
1.5 m
3 m
D Mid
m | s | sand | grav
1m
1.5 m
3 m
F
m | s | sand | grav
1.5 m
2.5 m
2 m
0.5 to 1 m
SW
Fig.11d
f3
f2
f1

Fig. 10

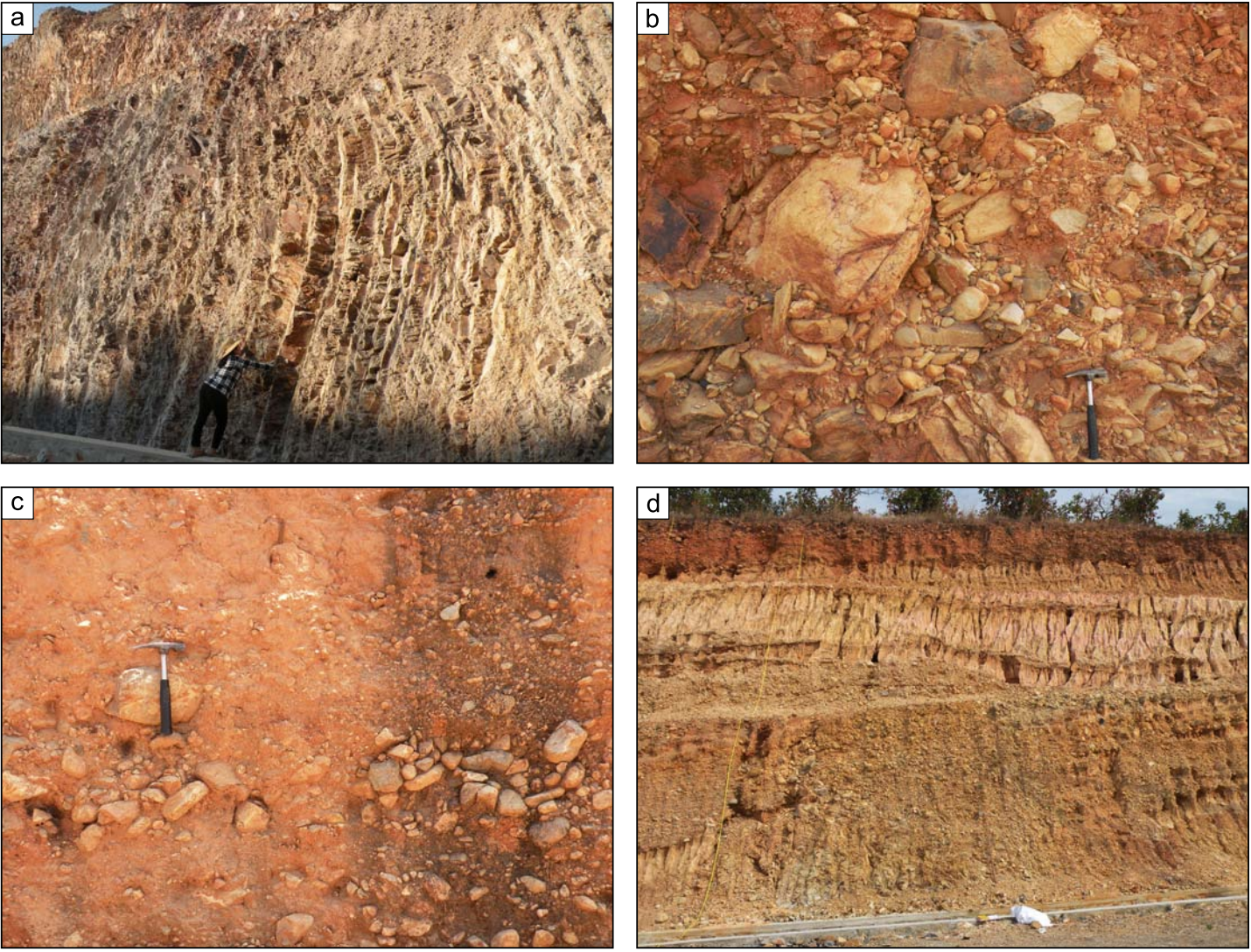

Fig. 11

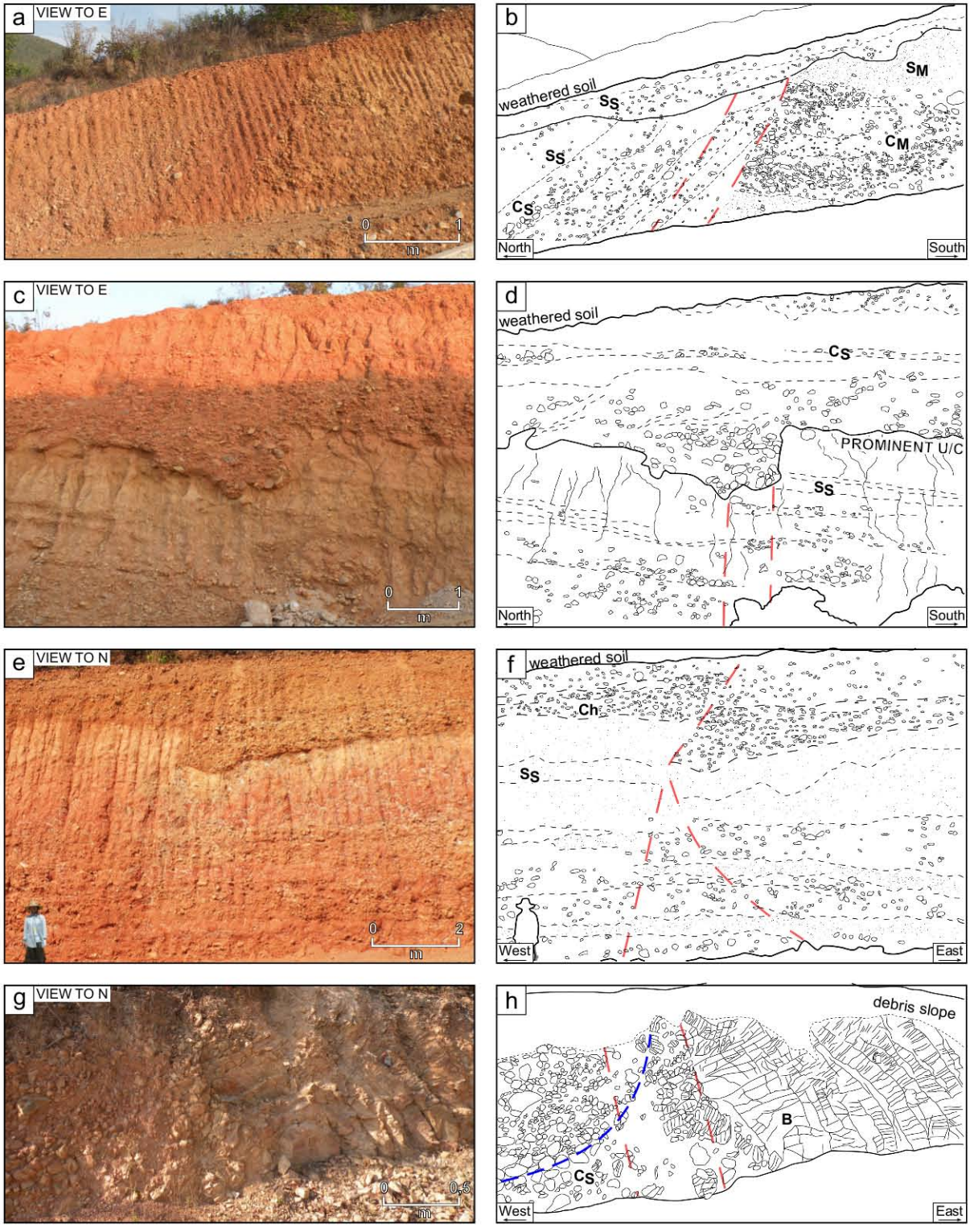
a
VIEW TO E
0
1
m
b
weathered soil
Ss
Ss
Cs
SM
CM
North
South
c
VIEW TO E
0
1
m
d
weathered soil
Cs
PROMINENT U/C
Ss
North
South
e
VIEW TO N
0
2
m
f
weathered soil
Ch
Ss
West
East
g
VIEW TO N
0
0,5
m
h
debris slope
B
Cs
West
East

Fig. 10 a-h

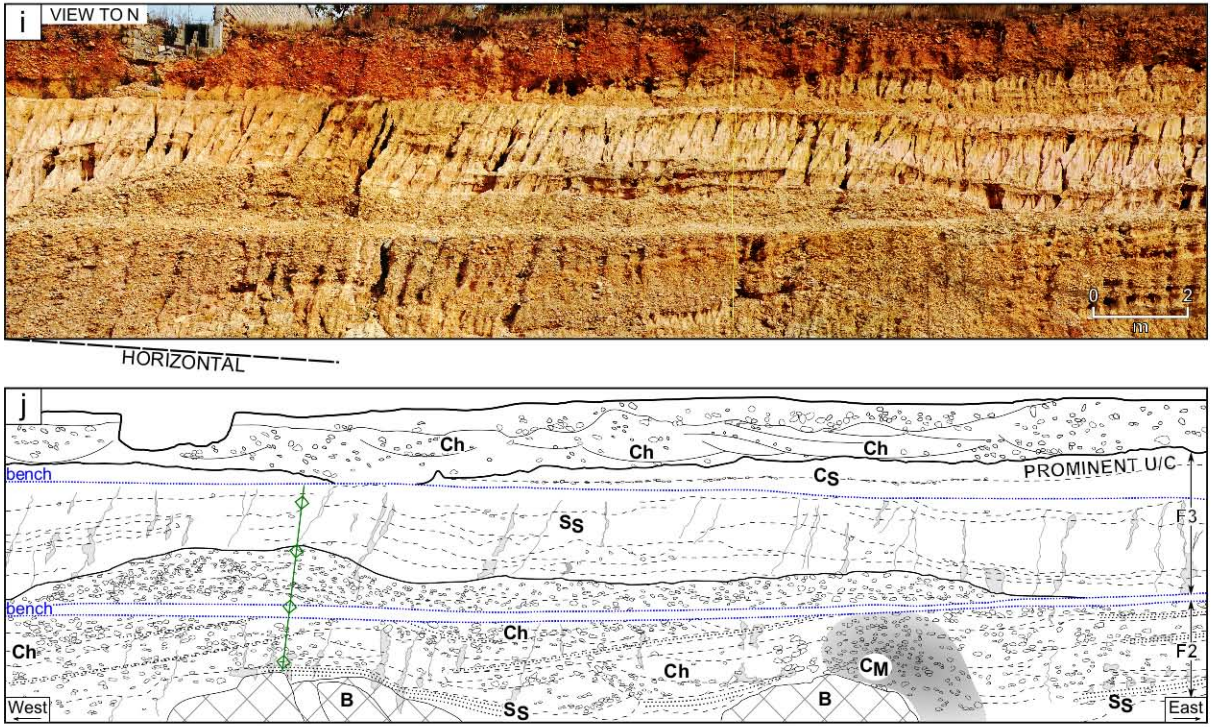
i
VIEW TO N
0
2
m
HORIZONTAL
j
Ch
Ch
Ch
Cs
PROMINENT U/C
bench
Ss
F3
bench
Ch
Ch
Ch
CM
F2
West
B
Ss
B
Ss
East

Fig. 10 i-j

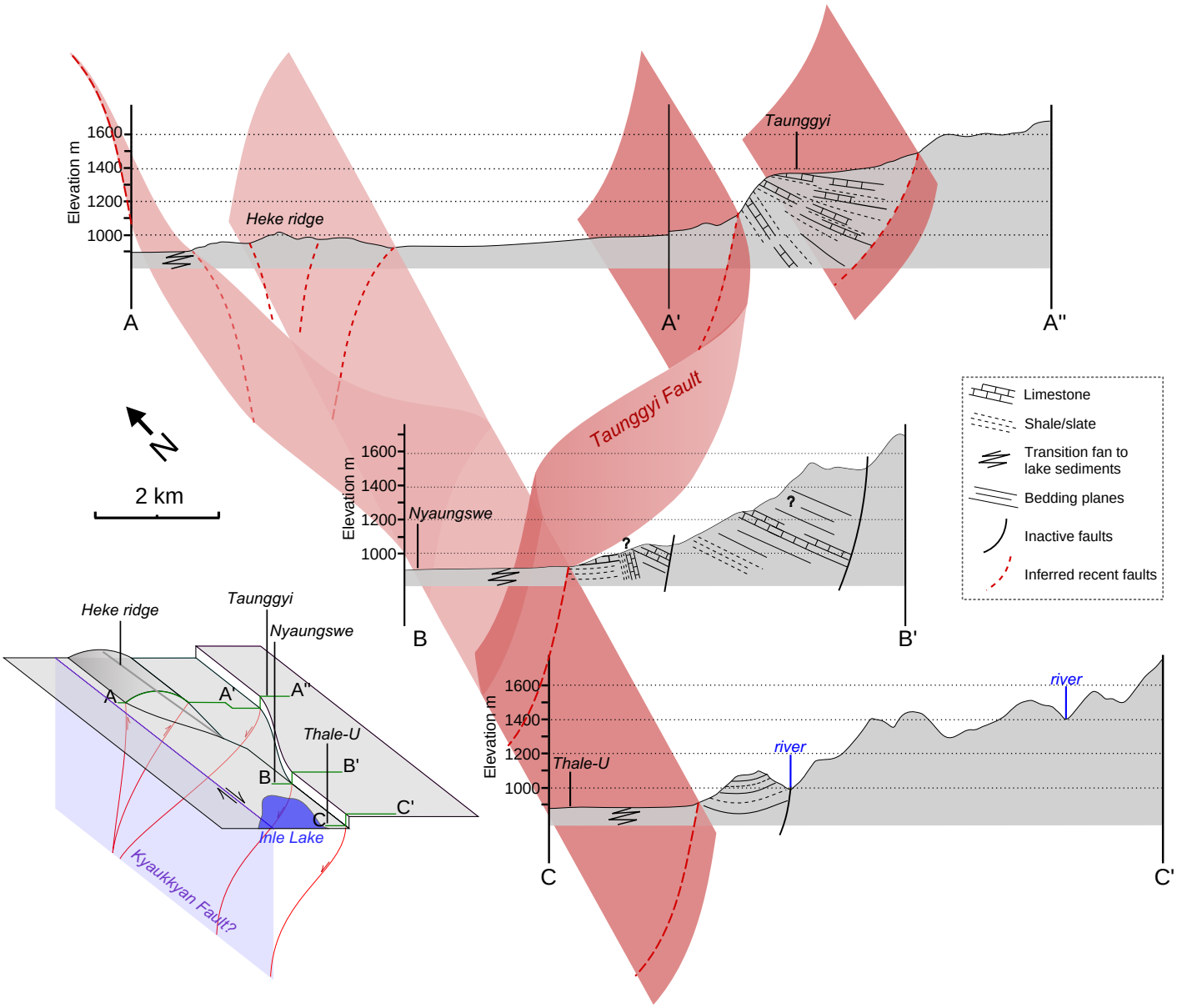
Elevation m
1600
1400
1200
1000
Heke ridge
Taunggyi
A
A'
A''
Taunggyi Fault
N
2 km
Nyaungswe
B
B'
?
Limestone
Shale/slate
Transition fan to lake sediments
Bedding planes
Inactive faults
Inferred recent faults
Thale-U
river
C
C'
Inle Lake
Kyaukkyan Fault?

Fig. 11